Projektantska skupina
2.TIR

Sofinancirano s pomočjo Instrumenta za povezovanje Evrope Evropske unije

IRGO CONSULTING d.o.o.

Technical report

Second track of the railway line Divača-Koper, Part 1
Drugi tir železniške proge Divača- Koper, Sklop 1

An object	**Tunnel T1 and T2**	
Part of the object/ Content	**GG elaborate for tunnels T1 and T2**	
Project number	**190175/1**	
Design number	190175/1-E/02	
Project type	PZI (execution design)	
Project manager	Angelo Žigon, univ. dipl. inž. grad.	G-0680
Project manager deputy	dr. Vojkan Jovičić, univ.dipl.inž.grad.	G-2103
Chartered engineers	dr. Vladimir Vukadin, univ.dipl.inž.geol. Julija Fux, univ.dipl.inž.geol.	RG-0099 RG-0160
Authors	dr. Vladimir Vukadin, univ.dipl.inž.geol. Julija Fux, univ.dipl.inž.geol.	RG-0099 RG-0160
Design status	approved	
Version	003	
Date	junij 2020	

SŽ - Projektivno podjetje d.d.
Ukmarjeva ulica 6,
1000, Ljubljana

Elea iC d.o.o.
Dunajska cesta 21,
1000, Ljubljana

IRGO CONSULTING d.o.o.
IRGO consulting d.o.o.
Slovenčeva ulica 93,
1000, Ljubljana

Table of contents

Figures

Tables

Annexes

1 GENERAL

1.1 Introduction

The project for the construction of the second track between Divača on Koper (2TDK) is an integral part of the Trans-European Transport Network and envisages the construction of a 27.1 km new railway line. The new line foresees the construction of eight tunnels, two viaducts, two bridges, one gallery, with 75% of the route running in tunnels (20.5 km).

An overview map of the object route is given in the figure below. More detailed project information is available on the project portal.

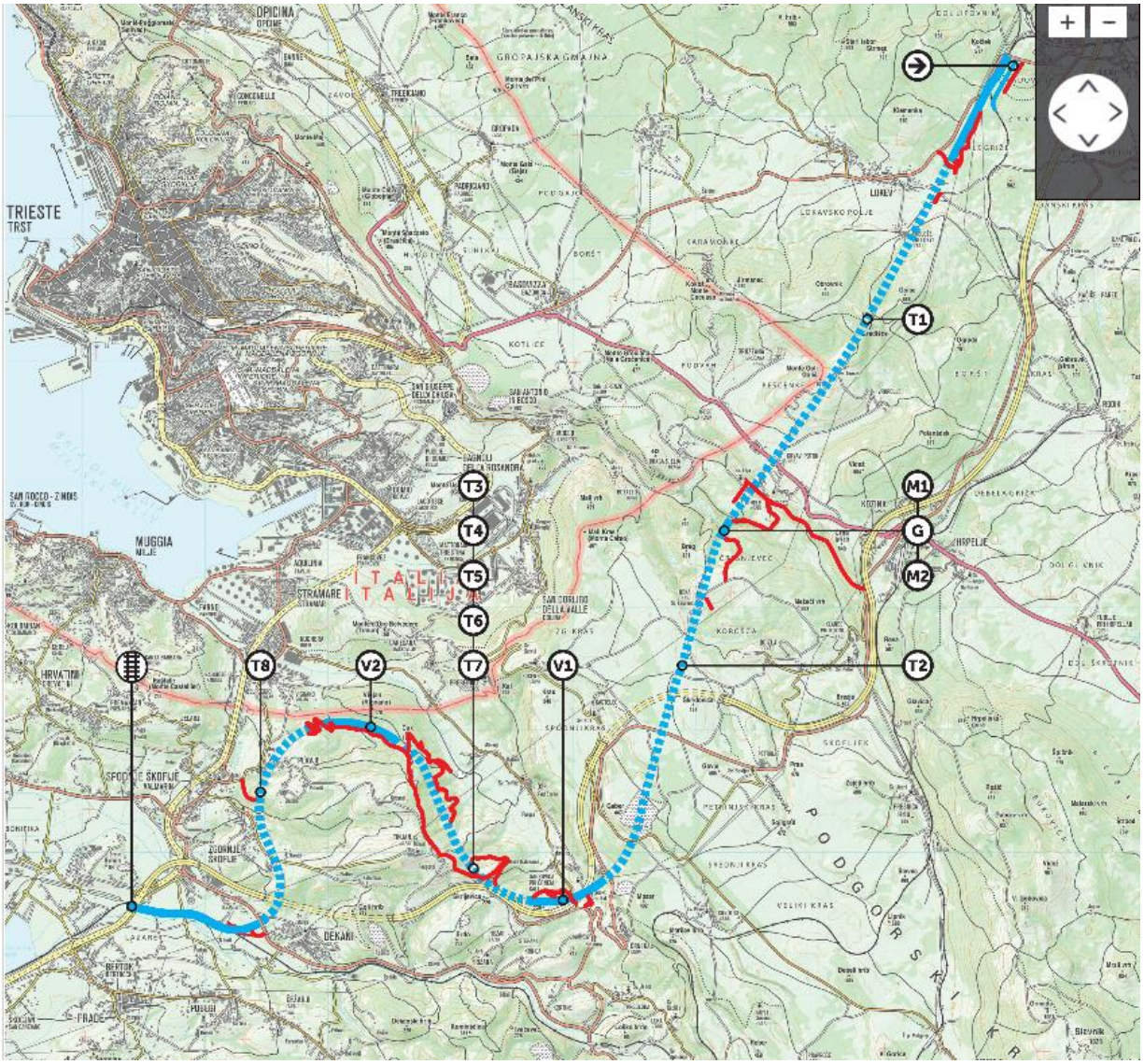

Figure 1: An outline of the situational course of the route (http://www.drugitir.si/en/second-track/)

For the purpose of the project, the route is divided into two lots: Lot 1 (km 00+000 to km 15+945.6), which runs in the direction of NNE-SSW, mainly along with the karst terrain built by limestone, and in smaller part by flysch rocks, Lot 2 (km 15+945.6 – km 28+056.2) is entirely covered by flysch rocks developed below the Karst edge.

This GG study presents a synthesis report (PZI – detailed design phase) for both tunnels T1 and T2, located on Lot 1. It is based on studies produced in the period from 2010 to 2018 and references [1] to [8]. These sources provide all the results of structural geological, paleontological, sedimentological, hydrogeological, karst, geophysical, geotechnical investigations, borehole's logs, lab tests, etc.

In the preparation of all the documents listed in references, experts from different companies participated, by fields, as indicated below:

-Designing structural-geological map of a broader area:	GeoZS (PGD, PZI)
-Designing a karst base:	IZRC SAZU (PGD, PZI)
-Execution of geophysical tests:	Geoinženiring in Pöyry (PGD)
-Execution of geo-radar tests:	Bo-Ra-tec and ZRMK (PGD, PZI)
-Execution of borehole logging:	GeoZS and Fugro (PGD, PZI)
-Execution of lab tests:	IRGO Consulting, ZAG and Geoportal (PGD, PZI)
-Execution of field geotechnical measures:	IRGO Consulting, FGG-KMTal in Econo (PGD)
-Execution of hydrogeological measures and tests:	IRGO Consulting, GeoZS (PGD, PZI)
-Execution of drilling:	Crossco, Imprefond and Rovs (PGD), Geotech S.p.A., Ground engineering ltd (PZI)

1.1 General about facilities

1.1.1 Tunnel T1

Tunnel T1 is the first and the longest of the eight tunnels in the railway line between Divača and Koper. The length of the main tunnel is 6,714 m, and the service tunnel 6,683 m, along with the route between km 2+966 and km 9+680, in the area between the settlement Lokev and the Glinščica valley.

Above the main and service tunnels, there are several other houses and outbuildings in Krvavi Potok, where the Kozina - Trieste state road crosses it. The thickness of the roof in this part is 133 m. The tunnel route crosses several other local roads, but the coverage is even more than a few tens of meters in these parts. The maximum coverage of 367 m reaches about one-third of its tunnel route, at a 5+735 m. In immediate vicinity of the service tunnel, in the area of Lokve settlement, at a 3+150 m chainage, there is a house which will suffer, by our expectations, at least the dynamic effects of blasting during tunnel construction.

We have designed the facility as a single-tube tunnel with an excavation profile of 70.36 m^2 on the undrained part and 73.00 m^2 on the drained part. On the left side of the main tunnel, there is a parallel service tunnel, whose illuminated profile is identical to the light profile of the main tunnel and provides access for trucks and ambulances. For the passage of people in the event of an accident, the main and service tunnels are connected to diameters at distances of no more than 500 m. The excavation profile of the widths is 58.21 m^2. In the area of the northern portal, the axial length of the service tunnel is 12.5 m, then it moves away from the main tunnel at approximately 25 m and remains the same at all times.

The northeren portal is dug-into over 20 m; before the entrance, the bottom of the dug-in is extended to 30 m, where the access road T-1a is connected. It connects the regional public road R1-205/1026 Divača - Lokev - Lipica. The tunnel then flows under a minimum cover of 10-15 m over a length of 130 m. In this part, the route crosses the local waterworks and access road. The southern portal is located in the steep slopes of the Glinščica valley. Between the portal of the main T1 tunnel and the end strut of the Glinščica 1 bridge is a plateau on a manmade fill of ca. 12 m wide and ca. 36 m, which extends to the plateau in front of the plateau of the service tube with a width of ca. 45 m and length approx. 45 m. The access road T-1b2 is connected to the plateau, which is connected to the access road T-1b1, which is via a local road about ca. 70 m long, and relates to the regional road R2 409/0311 Kozina - Kastelec.

Situationally, the tunnel route is given on the IG map in Annex G.1, and the longitudinal geological-geomechanical cross-section on Annex G.2.

1.1.2 Area between tunnels T1 and T2 (Glinščica)

For the needs of overcoming the Glinščica valley and for the needs of connecting tunnels T1 and T2, bridges Glinščica 1 and Glinščica 2 will be constructed, as well a gallery between them.

An area in front of the tunnels T1 and T2 (of length ca. 300 m) is not the subject of the works in the Call within Lot 1. We have gained some data during the investigations. Those we used for designing the constructions (bridges Glinščica 1, 2 and gallery Glinščica). We have made analysis and interpretations for both tunnel areas.

1.1.3 Tunnel T2

The T2 tunnel route runs in the direction of SSV - SW, with the total tunnel length of 6,017 m and service tunnel 6,028 m, located between km 9+928 and km 15+945 on the route between the Glinščica and Črni Kal valleys.

The surface above the route of the building is mostly without facilities, only in the northern part between the km 10+900 and 11+200 stations lies above the tunnel Beka. In the area of Beka settlement, the height of the roof varies between 130 and 145 m. At the km 12+700 chainage runs above the tunnel Kastelec, a highway Ljubljana-Koper, where the height of the roof increases to approx. 180 m, while the height difference between the motorway and railway tunnels is up to 110 m. At km 13+280, where we follow a similar overburden of approx. 185 m to Ljubljana-Koper highway. Between the km 14+300 and 14+850 chainage, the area of the Črnotiče quarry extends above the tunnel, with an elevation of between 175 and 190 m.

The facility is designed as a single-tube tunnel with an excavation profile of 70.36 m^2 on the undrained part and 73.00 m^2 on the drained part. On the left side of the main tunnel, there is a parallel service tunnel, whose illuminated profile is identical to the light profile of the main tunnel and provides access for trucks and ambulances. For the passage of people in the event of an accident, the main and service tunnels are connected to diameters at distances of no more than 500 m. The excavation profile of the widths is 58.21 m^2. In the area of the northern portal, the axial length of the service tunnel is 12.5 m, and then it moves away from the main tunnel at approximately 25 m and remains the same at all times.

The northern portal of the tunnel is cut into the slope of the torrential ravine of the Glinščica stream. Between the portal of the main T2 tunnel and the end strut of the bridge Glinščica 2, there is a plateau on a manmade fill with a width of ca. 10 m and length approx. 27 m. In front of the T2 service tunnel portal, there is a plateau on a manmade fill with a width of ca. 20 m and length approx. 12 m. The access road T-2a is connected to the plateau, which through the network of local roads, relates to the regional highway R2 409/311 Kozina - Kastelec. The construction of the 53 m wide and approx. 240 m long rescue plateau at the bottom of the dug-in. The width of the bottom of the dug-in allows entry into the main and service T2 tunnel. Until the entrenchment in front of the T2 tunnel portal, the access road T-2b will be connected to the public local road Gabrovica - Črni Kal, which is adjacent to the regional road R2 409/312 Kastelec - Črni Kal.

Situationally, the tunnel route is given on the IG chart in Annex G.1, and the longitudinal geological-geomechanical cross-section on Annex G.2.

2 THE INVESTIGATIONS CARRIED OUT

This chapter presents a brief description of all investigations carried out in the area of both tunnels. Detailed descriptions of all tests with results are in references [1] to [8].

2.1 Structural-geological mapping and analysis

They performed structural-geological mapping and analysis of the broader route area of track II. Activities included analysis of existing data, terrain and borehole mapping, geomorphological analysis, lab testing, and the use of all relevant other data (e.g., geophysics) in the interpretation and setting of the lithostratigraphic and structural model of the investigated area. Based on these activities, an IG map (Annex G.1) and longitudinal geological sections along with the axes of tunnels T1 and T2 (Annex G.2) were created, which formed the base for other interpretations. The progress of the investigations with results and references to other studies and surveys used is given in reference [1].

2.2 Karst review and analysis

A karst survey and analysis of the track II broader area was carried out. Activities included: analysis of existing data, terrain mapping, caves, boreholes, geomorphological analysis, implementation of monitoring (hydrogeology) of the Beško-Ocizelj cave system with surface water supply (sinkholes), hydrogeology of karst springs in the impacted area T1 and T2, and tracing experiments and determination of nitrates in the filled karst portions of the boreholes. Based on these activities, karst prevalence in the area of tunnels T1 and T2 was evaluated. The progress of the investigations with results and references to other studies and surveys used is given in reference [1].

2.3 Exploration drilling and excavation

Boreholes and excavations were performed primarily to determine GG conditions and to take samples. Boreholes and excavations were geological, IG, HG, and karst mapped, borehole cores were photographed, and samples were taken for lab testing. Most of the borehole cores are stored in the Geological Survey Facility. The boreholes were subjected to pouring tests, pressiometric measures, SPT tests, logging, geo-radar, and video recording. Specific boreholes were fitted as piezometers or inclinometers, and all boreholes were surveyed. Their locations are shown on the engineering-geological map in Annex G.1, and the GG inventories are given in Annex G.3.

Detailed drilling and excavation logs for T1 and T2 tunnels are given in references [1] to [6] and for the Glinščica area in references [7] and [8].

2.3.1 Tunnel T1

In the T1 tunnel area, seventeen boreholes were drilled at a total depth of 1.401 m, of which five deep boreholes totalled 1.035 m in length and twelve shallow boreholes in the northern and southern portals with a total length of 366 m. In the area of portals, we also carried out two excavations with a backhoe.

During the supplementary survey (PGD_{dop}), four deep boreholes with a total length of 1.060 m were conducted in the T1 tunnel area. Individual sections of the boreholes were drilled to the core using a double-core, and the remaining parts were drilled using non-core destructive drilling. The sections were determined based on known structural-geological data and with an emphasis on obtaining data in more complex parts for each borehole. Primary data on boreholes are given in Annex P.1., while GG borehole logs are given in Annex G.3.

2.3.2 Tunnel T2

In the T2 tunnel area, fifteen boreholes were drilled in the basic design (PGD) phase at a total depth of 1.965 m, of which nine deep boreholes in a complete length of 1.840 m and six shallow boreholes in the northern portal area in an entire range of 155 m. In the area of the portals, we also carried out three excavations with a backhoe.

During the supplementary survey in the detailed design (PZI), five deep boreholes, with a total length of 1.050 m, were conducted in the T2 tunnel area. Individual sections of the boreholes were drilled to the core using a double-core, and the remaining parts were drilled using non-core destructive drilling. The sections were determined based on structural-geological data and with an emphasis on obtaining data in more complex parts for each borehole. Primary data on boreholes are given in Annex P.1., while GG borehole logs are given in Annex G.3.

2.3.3 Area between tunnels T1 and T2 (Glinščica)

In the area between tunnels T1 and T2 (Glinščica), seventeen holes were drilled in a total depth of 300 m. The boreholes were drilled geomechanically. Primary data on boreholes are given in Annex P.1., while GG boreholes logs are given in Annex G.3.

2.4 Engineering-geological (IG) mapping and analysis

Within the framework of IG mapping and analysis, the following activities were carried out: geomorphological analysis of stereo models from aerial photographs, IG mapping of the terrain, records of rock mass outcrops, records of labile zones, weathering and weathering depth determinations, discontinuity incidence measures, GSI and RMR index estimations of a rock mass. Within the framework of engineering-geological mapping, we thoroughly surveyed the boreholes cores. We determined the RQD, the degree of damage; we recorded the cracks (incidence, fill, intensity), established the GSI and RMR values, and finally determined the GT and BT units that occur in the tunnel area.

2.5 Hydrogeological research

The following examinations and measures were carried out to determine the hydrogeological conditions in the T1 and T2 tunnel area:

- hydrogeological mapping,
- hydraulic testing in boreholes,
- equipment of selected boreholes with piezometers,
- equipment of piezometer boreholes with an automatic water-level recorder to monitor groundwater level and temperature,
- filling experiments in boreholes,
- borehole water sampling for chemical testing.

All details of the investigations carried out with the results are given in references [2], [3], [4], [5], [6], [7] and [8].

2.5.1 Measures of surface watercourses

Within the framework of the HG monitoring setup, continuous measures of water level in the riverbeds of the following streams are carried out: Škofije stream, Glinščica, Plavje stream, Griža.

All data on the performed hydrogeological flow measures are given in reference [1].

2.6 Geomechanical field survey

The field survey was carried out during the basic design (PGD) phase to investigate the situation in the area of both tunnels. Below we present the investigations carried out in the area of T1 and T2 tunnels and the valley of Glinščica:

- pressiometric measures using OYO Elastmeter 2,
- SPT tests (shallow boreholes, portals),
- measures with seismic flat dilatometer (portals).

In the PGD_{dop} phase, no additional field geomechanical investigations were performed. All details of the studies carried out with the results are given in references [2], [3], [4], [5], [6], [7] and [8].

2.7 Geomechanical lab tests

Several lab tests were performed on the cores of samples taken from the boreholes. The following is an overview of the investigations carried out in the area of T1 and T2 tunnels and the Glinščica valley.

The following lab tests were carried out at the cores of the rock samples:

- volume weight,
- uniaxial compressive strength,
- rock solidity in a triaxle stress state,
- measures of Young's elastic modulus and Poisson's ratio,
- measures of dynamic properties,
- tensile strength,
- shear strength,
- resistance investigations.

The following lab tests were carried out at the cores of soil samples:

- volume weight and moisture,
- sieve analysis,
- consistency and plasticity tests,
- direct shear tests,
- EC and USCS land classification.

All details of the investigations carried out with the results are given in references [2], [3], [4], [5], [6], [7] and [8].

2.8 Groundwater testing towards aggressiveness

The following parameters were determined on ten water samples:

- temperature and conductivity,
- smell,
- sulphate, pH,
- aggressiveness of CO_2, ammonia, Ca, Mg, Na, K^+ and Cl^- and NO_3^{2-} ,
- aggressiveness of water to concrete.

The results are summarized in references [2] to [6].

2.9 Geophysical investigations

The subsequent geophysical investigations have been carried out in the tunnels T1 and T2:

- video recording and logging of boreholes,
- optical recording,

- geo-radar measures in boreholes,
- seismic refraction,
- electrical tomography,
- vertical electrical sounding.

All result details are given in references [2], [3], [4], [5] ,and [6].

3 STRUCTURALLY GEOLOGICAL CONDITIONS

3.1 Lithostratigraphic units

This chapter describes all lithostratigraphic units as superpositioned from the bottom up in the investigated territory. We used the formation principle when describing lithostratigraphic units. The fundamental unit is the formation, which is characterized primarily by lithological homogeneity, and sedimentological and paleo ecological features as well. The latter is the product of a single sedimentation area and thus associated with approximately uniform physical properties of the rock body. An essential criterion for the classification of lithostratigraphic units in the investigated territory was that they were sufficiently recognizable in their characteristics and could be monitored laterally and vertically in the field.

The individual units are briefly summarized below, as their detailed description is given in reference [1] and are shown spatially on the IG map (G.1) and longitudinal profile (G.2).

3.1.1 Sežana Formation (SF/K2-42) - Cretaceous

In the most northern part of the surveyed area between km 0+000 and km 1+700 western of Divača, the upper part of the Sežana Formation is issued. The limestone of the Sežana Formation is mostly medium to thickly layered, olive-bearing biomicrite, and pelbiomicrite. Locally, thin, up to several meters (and less) thick packages of the dark grey flat and laminated limestone appear between the layered limestones.

The age of the Sežana Formation based on the microfossil assemblage comprises part of the Turonian, Coniacian, and Lower Santonian but only the younger one, i.e., the Santonian part of the formation, is developed in the studied area. The thickness of the Sežana Formation on the broader field of the Trieste - Komen plateau ranges from 230 to 500 m and is about 450 m thick in the studied area.

3.1.2 Lipica Formation (LF/K4-52) - Cretaceous

The layers of the Lipica Formation (between km 1+700 and km 2+700) usually lie on the Sežana Formation, above which the Liburnian Formation was deposited after a short emergence phase. The transition between the Sežana and Lipica Formation is gradual, so it is not very easy to draw a precise boundary between them. An essential type of limestone of the Lipica Formation is light grey, thick-layered to massive biomicrite to biosparite (bioclastic floatstone) with partially or entirely washed micrite base.

The age of the Lipica Formation on the Trieste - Komen plateau includes the upper part of the Santonian and the lower part of the Campanian. Only Upper Santonian layers have been developed within the studied area. An outcrop has already been recorded in the Campanian in this part of the Karst. The thickness of the Lipica Formation in the study area is 350 m.

3.1.3 The Karst unit

Upper Cretaceous (Maastrichtian) and Paleogene (Palaeocene and Eocene) platform carbonates (Liburnian Formation, Trstelj Formation, Alveolina Nummulitic limestone) form the Karst unit, which is a higher-order lithostratigraphic unit and the final mega sequence of the Adriatic-Dinaric Carbonate. The lower boundary is represented by regional discordance, and above the unit, it is bounded by the basin clasts, which indicate the sinking of the carbonate platform. The Karst unit is composed of hundreds of meters thick sequences of paralysis and shallow-water carbonates. This chapter describes only those characteristics of individual Formations and members of the Karst unit that are necessary for a fundamental understanding of the geological structure of the studied area.

3.1.3.1 Liburnian Formation (LIB/K-Pc) - Cretaceous-Palaeocene

After discontinuation of sedimentation, freshwater, brackish, and shallow-water carbonates of the Liburnian Formation began depositing on the Santonian-Campanian carbonates of the Lipica Formation above the pronounced Paleocracian horizon. The upper boundary of the formation is represented by the transition to the thick and massive bioclastic limestones of the lower part of the Trstelj Formation (= Lower Trstelj beds).

The Liburnian Formation in this part of the Karst is generally considered to be limestone of the lower part, i.e., Vremščica facies, layered, medium to dark grey in color, biomicrite and pelmicrite in structure. The thickness of the Liburnian Formation at Lokve is estimated at more than 300 m and probably does not exceed 150 m in the territory of Krvavi Potok.

3.1.3.2 Trstelj Formation (TF/Pc) - Paleocene

Above the Liburnian Formation lie different types of deadpan-layered bioclastic limestones of the Lower Trstelj beds. By structure, washed-out biopelmicrite or intrabiomicrite (wackestone and packstone, often grainstone) predominate in the Lower Trstelj beds. The thickness of the Lower Trstelj beds at Prelože is up to 150 m maximum and at Krvavi Potok, about 100 m.

As a rule, in the lowest part of the Upper Trstelj beds lies light grey to white massive coral-algal limestone. It outcrops in individual differently thick lens bodies throughout the territory of the Trieste-Komen plateau. The more significant part of the Upper Trstelj beds is characterized by poorly layered to massive light grey bioclastic limestone (mainly packstone and wackestone). The thickness of this section at Prelože is up to 100 m, while it reaches a maximum of 50 m in the area of Krvavi Potok.

3.1.3.3 Alveolina Nummulitic limestone (ANA/E) - Eocene

Above the Trstelj Formation lie indistinctly layered locally massive Alveolina Nummulitic limestones, which belong to the youngest formation of the Karst unit and, at the same time, the final lithostratigraphic unit of the carbonate development of the Dinaric carbonate platform. Alveolina Nummulitic limestone is followed from the bottom up by Alveolina limestone, Nummulitic limestone, and limestone. It is predominantly light grey to white, sometimes dark grey, medium to thick; layering is weakly expressed. The upper limit of Alveolina Nummulitic limestone is sharp or gradual. When it is severe, limestones cross the Transitional layers through a pronounced hardground with basal conglomerates, and the transition may also be continuous so that layers of re-sedimented carbonates begin to emerge between the limestones and single horizons of marl limestones start to prevail.

Given that the thickness of the Alveolina Nummulitic limestone is not constant, the local development in the Formation also differs from one another. The Transitional layers are located within the limestone in the area of T1 tunnel at the level between km 5+550 and 6+650 in the syncline at Polanšček (Videž), between km 8+650 and 8+900 in the field of Krvavi Potok, Nasirc and Mihel (SV part of the Ocizelj brachisyncline). They were also located in T2 tunnel between Beka (the area of the Beško Ocizelj cave system) in the SW part of the Ocizelj brachisyncline. Then also were located in the predominant part of the thrust system to Črni Kal, except for the narrow belts below the thrust fault system where the direct contact of Alveolina Nummulitic limestone with Transitional layers is visible on the surface in several places: km 5+500, 6+500, 8+875, 11+490, 14+050, 15+090.

3.1.4 Transitional layers -conglomerate, marlstone, marl limestone, limestone (PP/E) - Eocene

The Transitional layers represent the formation of medium to thin-layer darker pelagic and hemipelagic marl limestone (packstone and wackestone) and marlstone, occurring between the Alveolina Nummulitic limestone in bedrock and the true flysch in the surface cover. A high proportion of planktonic foraminifera and echinoderm detritus characterize the Transitional layers, in addition to glauconite. The Transitional layers also contain pyrite, as individual smaller nests up to 1 cm in diameter, but more often present as a thorn in the fracture (thrust system)

surfaces. We propose to consider the effect of sulfuric acid generated by pyrite oxidation on the concrete lining of tunnel sections passing through the Transitional layers. The Transitional layers are classified by geological time in the Eocene (Ypresian and part of Cuisian).

The thickness of the Transitional layers varies greatly, but it is sometimes difficult to define its upper boundary at the flysch transition, especially if mainly the marl horizons occur in flysch. They also extend into a relatively wide belt southern of Beka, where they reach considerable thickness, but their increased thickness may also be the result of duplication at a thrust fault system. On their contact with the Alveolina Nummulitic limestone, caves of the contact Karst of the Beško-Ocizelj cave system developed. Some of the entrances to the caves (e.g., Jurjeva Cave) are developed directly at the contact. On the other hand, others are slightly displaced as they have developed due to the denudation of the relief.

3.1.5 Flysch (F/E) - Eocene

Flysch is characterized by the alternation of marlstone, siltstone, and lithic sandstone with layer thicknesses in different proportions corresponding to sedimentation conditions in the flysch basin. Sometimes thin layers of limestone are also present. The sandstone, dominated by quartz and feldspar grains, gradually transitions into alevrolite.

In the mapped area, the thickness of the layers generally varies from less than 1 cm in marlstones to a maximum of 1.5 m in sandstones. The thickness ratio of the marlstone and sandstone layers varies, as does the average thickness of the individual layers. In general, rock strength increases with higher granulation.

The route runs through flysch layers in the area of the brachisyncline of Veliko Gradišče on an area of km 5+500 to km 5+950. The flysch of Gradišče lies in large part concordantly over the Transitional layers, except on the eastern wing of the brachisyncline of Velika Gradišče, where a robust geological fault in the N-S direction separates it from Alveolina Nummulitic limestone. Due to the rapid weathering and overgrowth of the terrain, outcrops from marlstone and clayey marls are scarce. In past, they were subjected to strongly tectonic activity due to the proximity of the geological fault. The latter exists in the eastern brachisyncline wing. The thickness of the flysch in the brachisyncline of Velika Gradišče probably does not exceed 100 m anywhere and remains in the lowest part at least 150 m above the planned tunnel.

In the area of the Ocizelj brachisyncline there are strongly folded flysch layers from km 8+975 to km 11+280. Somehow, up to km 9+500, marlstones and siltstones alternate with sandstones in the ratio of 40:60, then up to km 10+500 sandstones dominate, some layers reach a thickness of up to 1.5 m, and on average up to 0.4 m thick layers. Among the sandstones are marlstones and siltstones in subordinate depth. In some areas, up to 5 m, thick marlstones inputs occur, but their lateral distribution cannot be ascertained due to relatively poorly visible outcrops outside the ravine. From km 10+500 onwards, the ratio of marlstones and siltstones towards sandstones is approximately 40:60. Flysch marlstones above the Transitional layers can be found on the surface at km 14+000, but outcrops are very rare there. Due to their geometry and structural conditions, they tectonically deflect relatively quickly in-depth, so the T2 tunnel does not cross them (see the section on the fundamental structure). Flysch marlstones are also found on the surface at km 15, and the T2 tunnel is supposed to intersect them at a station between km 14+050 and 14+300. The marlstones and siltstones appear on the surface at the southern portal of the T2 tunnel. Flysch is also building the entire Tinjan area, and the T8 tunnel will also be built-in flysch.

3.1.6 Rock fall blocks and colluvium sediments

Recent sediments include the newly discovered extensive colluvium of flysch rocks in the area of Veliko Gradišče. Also in a valley filled by colluvium at Mihele, where a new borehole T2-15/17 was made, submerged blocks on the steep slopes below the Črni Kal thrust fault in the area of the southern portal of the T2 tunnel, under the Socerb and Kastel thrust, consisting of Alveolina Nummulitic limestone. Recent sediments include colluvium in some

erosion ravines of flysch sandstone blocks too. Below the Kozina - Koper regional road, there is also limestone scree, which is probably of anthropogenic origin as a filler material in the construction of the road. Alluvium sediments cover the lower part of the Rižana valley. A prominent area of solid gravel of Alveolina Nummulitic limestone is also found in the western slopes of the Griža stream ravine.

3.1.7 Travertine

In the riverbeds, tributaries of Glinščica and in the area of the Plavje and Škofije streams, more or less thick crusts of travertine occur in flysch areas, mostly in steeper areas and waterfalls. The travertine is relatively compact.

3.1.8 Filling of karst caves, sinkholes

A cave corridor can be found at the turn of the service road behind the highway. It is located in the Alveolina Nummulitic limestone and filled by flowstone and sandy-silty sediment. It continues deep into the vicinity of the T2 tunnel level. In the sinkholes, there is a slightly more eluvium, partly of anthropogenic origin.

3.2 Structural complexity

The tunnels T1 and T2 run along with a structurally very complex territory, dominated by the thrust structure created by the displacement of reverse and thrust geological faults, with the Karst thrust edge created by the subversion of Istria under the Outer Dinarides while simultaneously rotating Istria towards the Outer Dinarides.

In the area of tunnels T1 and T2, in the direction of increasing chainage (as can be seen in the figure below) structural units are being followed one by another. First there is the brachisyncline of Veliko Gradišče, followed by the anticline of Vrhpolje. Then the brachisyncline of Ocizelj, the thrust fault of Petrinja, the thrust unit of Škrklovica, the thrust unit of Kastel, the thrust unit of Socerb, the thrust fault of Socerb, the thrust unit of Osapi, the thrust fault of Osapi, the thrust unit of Črni Kal, and finally the thrust fault of Črni Kal.

A detailed description of the structural conditions and units is given in reference [1] and is spatially presented on the IG map (G.1) and longitudinal profile (G.2). Each of these structural units was also discussed within the standpoint of geomechanical and hydrogeological conditions. The fact that the area is still exposed to active tectonic pressures in the NS or NE-SW direction is essential too. It implicitly indicates the course of the central horizontal in situ stress, which is probably at least 1.5 times higher than the vertical component (according to hydrofracturization data in the area tunnel T8 -Lot 2).

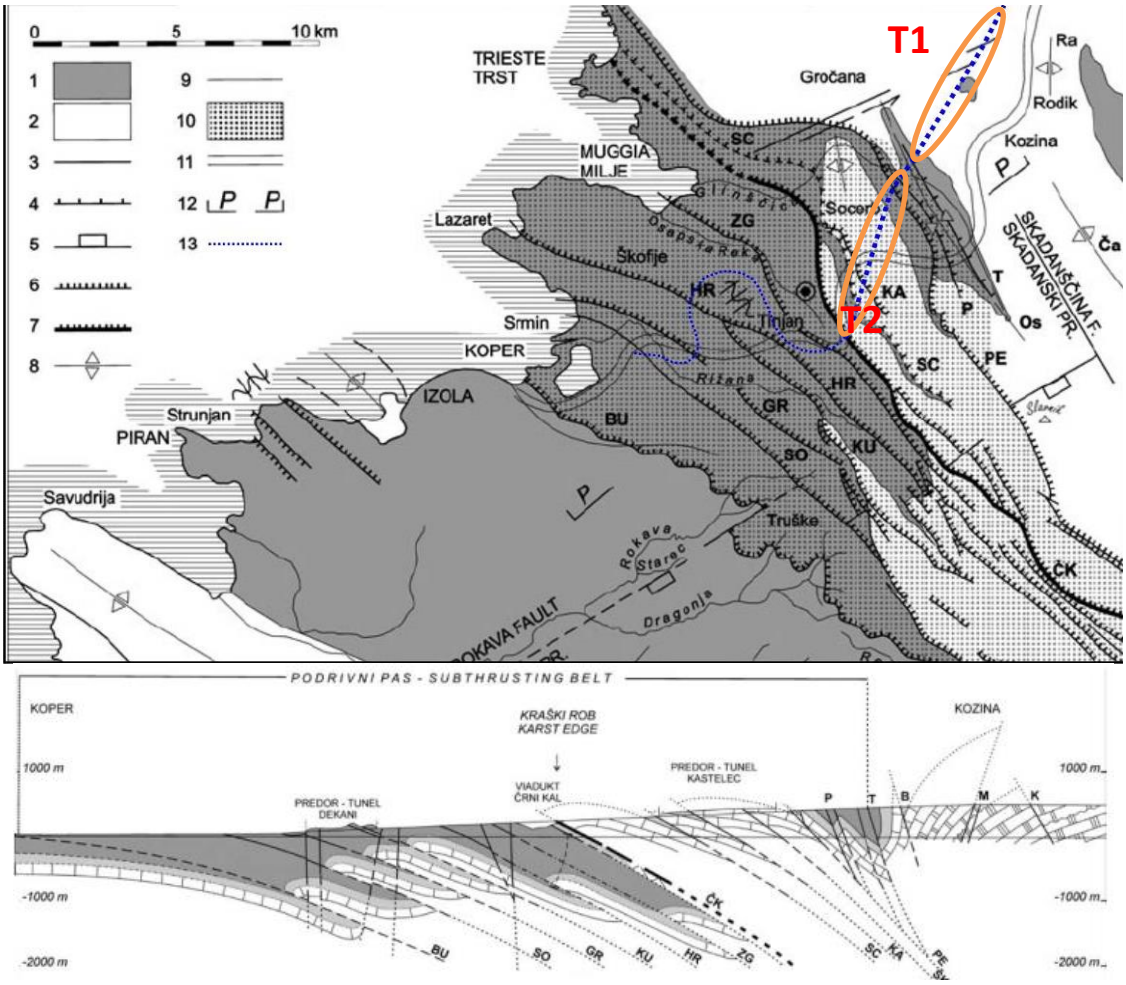

Figure 2: Tectonic sketch of the subduction zone, with an outlined route of the Divača – Koper track and major structural units (Placer, 2007)

4 KARST CONDITIONS

Details and interpretations of karst conditions are summarized in reference [1]. We provide a summary of the re-orientation of the route along with T1 and T2 tunnels in the figure below. It is divided into ten sections, as shown in the longitudinal sections in Appendix G.2.

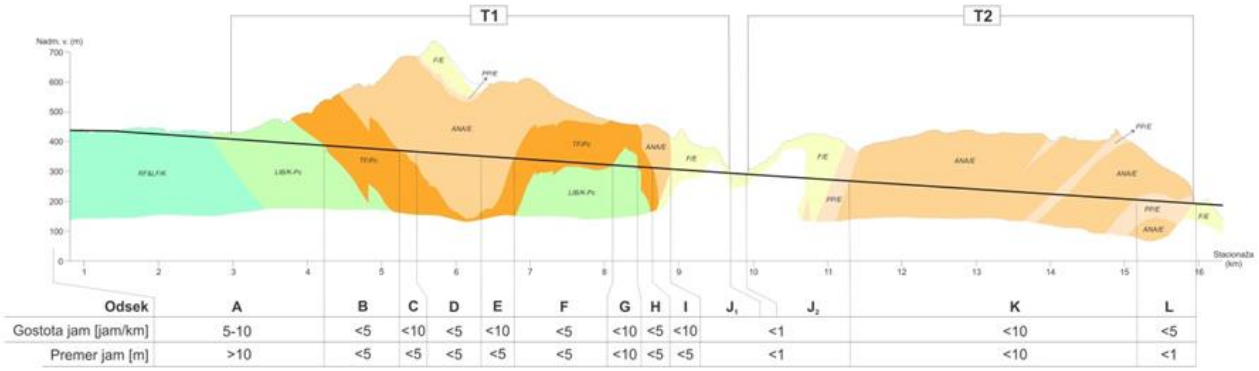

Odsek	A	B	C	D	E	F	G	H	I	J_1	J_2	K	L
Gostota jam [jam/km]	5-10	<5	<10	<5	<10	<5	<10	<5	<10	<1		<10	<5
Premer jam [m]	>10	<5	<5	<5	<5	<5	<10	<5	<5	<1		<10	<1

Figure 3: Predicted karst/perforated surface along with the tunnel route

Section A (km 0,00 - 4,23)

Section A runs along with the Cretaceous limestones and limestones of the Liburnian Formation. Cave corridors can be more abundant in diameter (even over 10 m). We expect that half to two-thirds of the cave corridors will be filled with fine-grained sediment and gravel (just below the surface), and more in-depth with the flowstone. (Sub) recent vadose abysses of up to 5 m in diameter in between may occur. The caves will be above the regional height of the karst groundwater, and in some places, we can expect jets that are more pronounced in the tunnel after rain and locally trapped water. Greater rock mass perforation is expected at the border between the Cretaceous and the Palaeocene layers, at the transition of section A and section B.

An average of 5 to 10 caves/km is expected, some with a diameter of over 10 m.

Section B (km 4,23 -5,24)

Section B runs through the Palaeocene limestones. Knowledge of lithology and borehole logs indicates a lower frequency of caves in these limestones. Most of the cave corridors are expected to be up to a few meters in diameter and will be filled with fine-grained sediments. Vadose abysses of up to several meters in diameter and several tens of meters in depth will also occur. The potential for trapped water is small but more extensive than in the previous section. More turbulence is expected on the shattered part at the chainage of km 4.69 and km 4.83.

Up to 5 caves/km up to 5 m in diameter are expected.

Section C (km 5,24 - 5,47)

Section C runs through the Eocene limestones and impermeable rocks do not cover them on the surface. These limestones are generally more subjected to karst activity, as indicated by data from the Črni Kal area.

Up to 10 caves/km up to 5 m in diameter are expected.

Section D (km 5,47 - 6,35)

Section D runs in the Eocene limestones but is covered by impermeable Eocene marls and flysch. Because carbonate rocks are covered with flysch, we do not expect vadose abysses. There is a higher possibility of locally trapped water in the area. We look for cave corridors of several meters in diameter, exceptionally even over 10 m, in the case of less expected remains of old, now relict caves.

Up to 5 caves/km up to 5 m in diameter are expected.

Section E (km 6,35 - 6,78)

Section E is equal to section C. Up to 10 caves/km up to 5 m in diameter are expected.

Section F (km 6,78 - 8,11)

Section F takes place in Paleocene limestones. Most of the cave corridors are expected to be several meters in diameter. Some caves may also be filled with sediment. Vadose abysses of up to a few meters in diameter are expected. According to the geological profile, it is likely that there will be more significant congestion at the fault zones at the km 7,090 and km 7,310 chainage.

Up to 5 caves/km up to 5 m in diameter are expected.

Section G (km 8,11 - 8,44)

Short section G runs through Cretaceous limestones. In this section, sections of more massive (sub) horizontal phreatic and epiphreatic caves are expected, the diameters of which can reach up to 5 meters. We also expect vadose abysses with a break of a few meters. A higher density of cave corridors is anticipated at the km 8.30 and km 8.44 chainage, as strong fault zones are expressed here.

Up to 10 caves/km up to 10 m in diameter are expected, in general.

Section H (km 8,44 - 8,65)

Section H runs through the Palaeocene limestones. Most of the cave corridors are expected to be several meters in diameter. Some caves may also be filled with sediment. Vadose abysses, up to a few meters in diameter, and upright, narrow, and long sprawling caves, formed at substantial faults and cracks of the JV-NW are expected. They can be up to 2 m wide and 10 m or more in length. More over-hollowness is anticipated at the chainage km 8.44, where the route crosses stable faulting structures.

Up to 5 caves/km are expected, on average, up to 5 m in diameter.

Section I (km 8,65 - 8,89)

Section I runs through the Eocene limestones. We expect vadose abysses of several meters in diameter. Higher degree of rock mass perforation we may expect at the contact of limestone with the Transitional layers and flysch at km 8.93 chainage.

In general, an average of 10 caves/km with a diameter of up to 5 m is expected.

Section J_1 (km 8,89-9,68)

Section J1 goes along with impermeable Eocene flysch rocks and the Transitional layers. Despite the considerable carbonate binder in flysch rocks, we do not expect any higher degree of perforation.

Up to 1 cave/km is expected, up to 5 m in diameter, in general.

Section J_2 (km 9,93-11,28)

The characteristics of section J2 are identical to section J1 (tunnel T1). Section J1 goes along with impermeable Eocene flysch rocks and the Transitional layers. Despite the considerable carbonate binder in flysch rocks, we do not expect any higher degree of perforation.

Generally, up to 1 pit/km in diameter up to 1 m occurs.

Section K (km 11,28-15,15)

Section K runs mostly through the Eocene Alveolina Nummulitic limestones with rare but essential hydrologically partially enclosed wedges of marl and flysch rocks. There are twenty cave entrances recorded within Karst cadaster in this section. The concentration of which is higher, especially between km 11,500 and 12,300 chainages (the Beško-Ocizelj cave system, relict epiphretic caves, and vadose abysses). In this section, more giant caves are

developed in the area of the Beško-Ocizelj cave system between km 11,280 and 11,800 chainages; here, the cave corridors also pass under the flysch overburden, from where the surface water flows.

It is expected the rock mass perforation in this section will be high; the diameters of relics and cave corridors will reach up to 10 m. There will also be relatively dense rock mass perforation with (sub) vertical vadose abysses up to 5 m in diameter. We expect more rock mass perforation at the Škrklovica thrust fault (km 12,520) and Kastel thrust fault (km 13,440); more karst zones are estimated at 200 m wide. A greater rock mass perforation of about 100 m into limestones is also expected along with the flysch husk of the Socerb thrust fault at km 14,020 and 14,210 chainages and along with the 200 m tunnel in the Alevolina Nummulitic limestones, where they rest on the Transitional layers (km 15,160). Under flysch husk, we can exclude the occurrence of vadose abysses. They are more likely only at the boundary of the overburden where the leaked water can flow beneath the overburden of the bedding plane.

At medium to low water levels, larger quantities of trapped water are expected between km 11,280 and 11,900 km (area of Beško-Ocizeljsko system). At high water levels, there are running water flows in the field, both below and above the height of the tunnel level. They run within flooding above the narrow cave corridors by at least 67 m above the tunnel level (e.g., the first retroversion cave corridor). However, there are also borehole conductive cave corridors (e.g., Cave corridor of large crevice), where even with 50 years of rainfalls, the water does not rise to the level of the tunnel.

Up to 10 caves/km are expected throughout the section, up to 10 m in diameter.

Section L (km15,15-15,93)

Section L runs through substantially impermeable Transition layers to which Alveolina Nummulitic limestones are deposited. The Osap cave, which is outside the immediate vicinity of the tunnel but directly above the Osap thrust fault in the zone of fluctuation of karst water level, indicates a relatively dense web of overflow cave corridors directly above the Osap thrust fault.

Due to the carbonate binder in the Transitional layers, only a slight overburden is expected, mainly in contact with the limestone. Due to the extremely flat, also horizontal and folded, Osap thrust fault, it is possible to catch trapped water along the entire route of this section.

Up to 5 caves/km with a diameter of up to 1 m is expected.

5 HYDROGEOLOGICAL CONDITIONS

5.1 Introduction

Data about past investigations and detailed interpretations of the hydrogeological conditions are given in references [1] to [5]. Further on, we present the main findings, which were focused on the assessment of water inrushes, the determination of maximum (peak) groundwater levels/pressures, and the determination of drained and undrained tunnel sections.

The key results are also summarized in the longitudinal section of Annex G.2.

5.2 Groundwater level fluctuation

5.2.1 Tunnel T1

The minimum measured and current levels, given in 2012, are similar to the current levels, measured as part of multi-annual monitoring until 2018. Low water drops below the tunnel level in piezometers T1-7/10 and T1-8/10 within the T1 tunnel route area. It has also been confirmed that the base level of karst groundwater is below the tunnel level at boreholes T1-7/10 and T1-14/17.

During rainfall, the level rises above the level in these piezometers too. Peak pressures were measured in borehole T1-7/10, where groundwater levels rise 99 m above sea level and fall 39 m below sea level in dry weather (the entire range of surface fluctuations is 137.80 m). Piezometers T1-8/10 and T1-10/10 show the occurrence of water overflows up to 30 and 40 above the level; otherwise, the groundwater level prevails between 15 and 25 m above the standard. It means that large quantities of karst groundwater are stored or streamed in this pressure zone above the level. The route of piezometric groundwater along with the T1 tunnel will be more reliable to define when measures of groundwater surface fluctuations at different water levels are available in the new piezometers T1-12/17, T1-13/17, and T1-14/17.

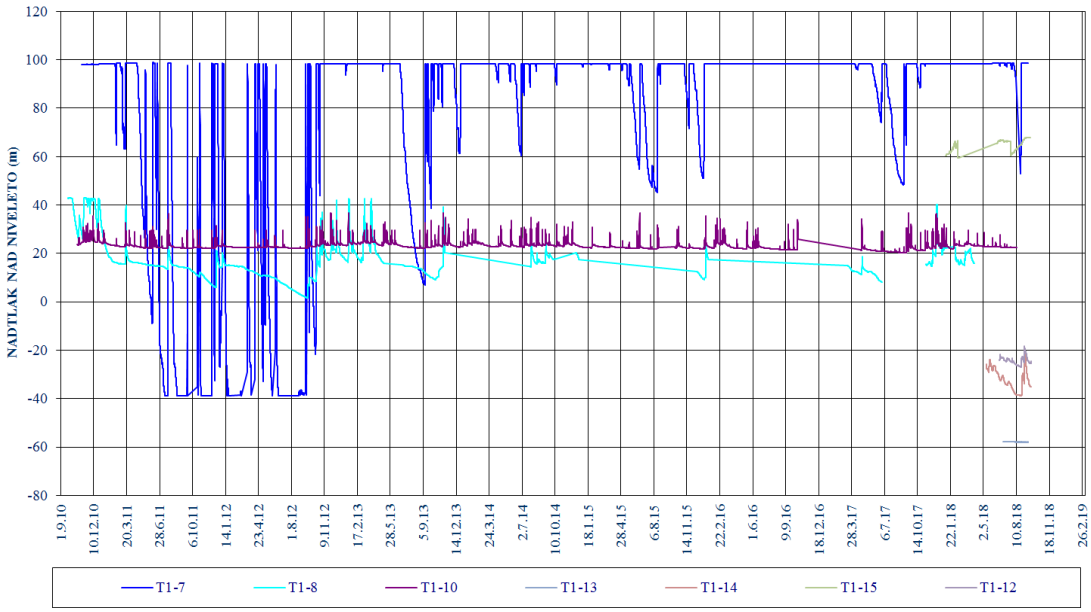

Figure 4: GVP fluctuations above/below the level (angle 0) in the tunnel T1

The measures made so far in the new piezometers show that in the central part of the syncline at the section between the 5+500 and 6+500 (ANA/E layers) groundwater levels even below the level of the T1 tunnel (borehole T1-13/17). It confirms our understanding of hydrogeological conditions and significantly improves the reliability of forecasts from previous interpretations (Figure 4). It is much more favorable for construction, but it is also the area of highest probability of occurrence of karst zones, where high karst waters may be expected to overflow.

The highest measured rate of pressure rise was in borehole T1-7/10, where the groundwater level increased by 68.80.m in one hour. Rapid pressure increases were also recorded at boreholes T1-14/17, T1-10/17, and T1-15/17, between 5-7 m/h.

5.2.2 Tunnel T2

A high groundwater level with a tip of 83 m above the level is in the area of the T2 tunnel in the piezometer T2-13 above the Črni Kal husk. The high peak level (72 m above the level) is also measured in the piezometer T2-9 near the Beško-Ocizelj cave system. In the T2-10 and T2-11 piezometers, which are characteristic of Alveolina Nummulitic limestones (ANA/E) between the Karst hinterlands of the Boljunca, and the Rižana and the Osap Rivers, the water level is at least 13 to 19 m below sea level at all times. At the outlet section of the T2 tunnel, the groundwater level in the piezometers T2-15 and T2-1 (south portal) is always about 20 m above the elevation angle, up to 43 m at high-water peaks and is connected to the outflow of water from the Karst system through the thrust contact of the Karst massive to the flysch layers. The groundwater level in the new borehole T2-16/17 is, on average, 151 m above the level, which is approximately 425.5 m above sea level, respectively 5 m below the surface.

Groundwater levels in boreholes T2-18/17 and T2-19/17 are below the tunnel level at the time of measures. Particularly low oscillation concerning the level can be expected in borehole T2-19/17, while in borehole T2-18/17, we can talk about the groundwater level in the levelling range. There are two measures in borehole T2-20/17, indicating that the groundwater level is between 23.6 and 40.0 m above the tunnel level, which is between 221 and 238 m above sea level.

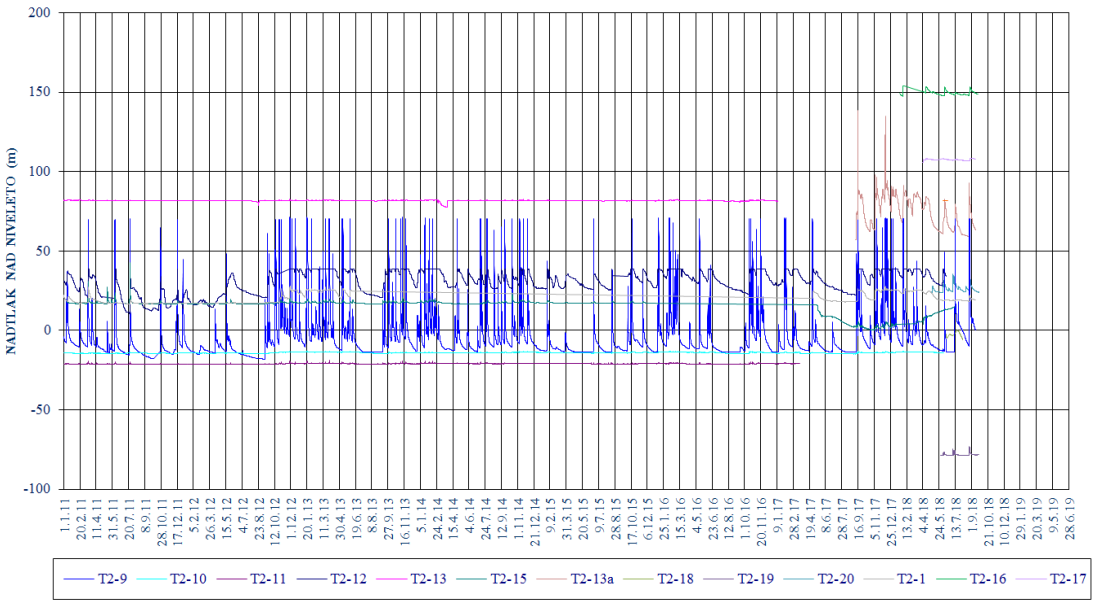

Figure 5: GVP fluctuations above / below the level (angle 0) in the tunnel T2

Piezometers (T2-9, T2-10, T2-11, T2-12, T2-13) cover the area of the T2 tunnel in Alveolina Nummulitic limestones. That occurs between the Škrklovica (T2-10), the Kastel (T2-12), and the Socerb (T2 -13) thrust faults. In the T2-13 piezometer area, the pressures are long-term high 80 m and represent more than 95% of the T2-13 measured

pressures. Short-term high strains occur still in the T2-9 piezometer in the area of Alveolina Nummulitic limestones, so we conclude that this is characteristic of Alveolina Nummulitic limestones in the T2 tunnel area. Pressure durations up to 40 m above the level are also long in the piezometer T2-12 in the central part of the tunnel in these layers. The T2-15 and T2-1 piezometers reach the Transitional layers at the base of the Črni Kal thrust zone, at the outlet section of the T2 tunnel. Here, pressures of 20 m above the level are long lasting (more than 99%), and they rise above 30 m for a maximum of several days.

5.3 Prevailing and maximum groundwater levels in tunnels T1 and T2

The longitudinal cross-section of the tunnel under consideration shows the highest measured and predominantly measured groundwater levels in all operating piezometers along the route. In the areas between piezometers, levels (as in the basic design (PGD) phase) are interpolated and partially interpreted according to a knowledge of permeability of the individual lithologic sections, taking into account the vertical expansion of the hydrogeological units and the depth of the tunnel level. In this way, the piezometric level along the entire tunnel under consideration is estimated.

Due to a more transparent interpretation of the distribution of the piezometric level within individual hydrogeological units, it is reasonable to consider the routes of both tunnels T1 and T2 together. As the karst fissure aquifers result in a markedly localized permeability increase within tectonically affected or karst zones, the pressure wave extends at a rate dependent on the resistance (inverted rate of the permeability) of the porous medium upon infiltration of precipitation and generally vertical drainage. As a result, rapid jumps in piezometric pressures may occur along relatively small distances. As such, pressure jumps may occur along with the known thrust structure, and preferential runoff paths in the vertical direction. The fact that in the addressed area we are dealing with this localized pressure system along the level, is evident from the analysis below.

In the area of tunnel T1, the course of piezometric levels in the basic design (PGD) phase was predicted in 2012, as shown by the grey broken line at the bottom of two diagrams with the scale on the right of the diagram (Figure 6 - maximum levels, Figure 7 - dominant groundwater levels). A light blue line (with a scale on the right) indicates the progress of the piezometric levels forecast in this report after the completion of the supplementary examinations.

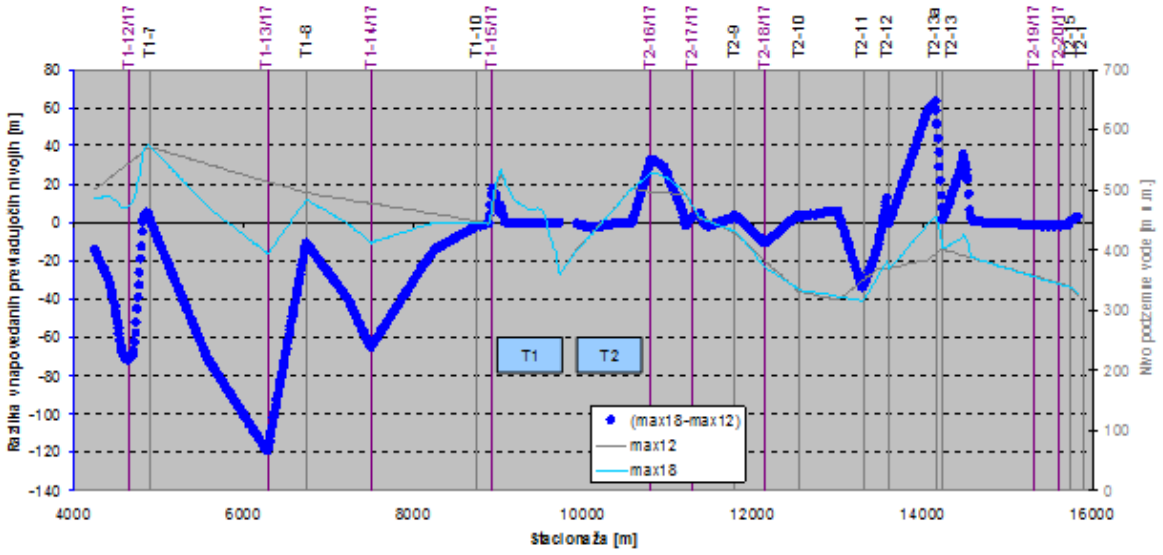

Figure 6: Difference in the prediction of maximum groundwater levels in the PGD (2012) and PZI (2019) phases

The difference between the two forecasts is given by the thicker dark blue line (with the scale on the left side of the diagram), with negative values indicating lower newly predicted levels and positive values indicating higher

new forecasts. Grey vertical lines indicate the position of the older piezometers, and purple vertical lines indicate the position of the additional piezometers.

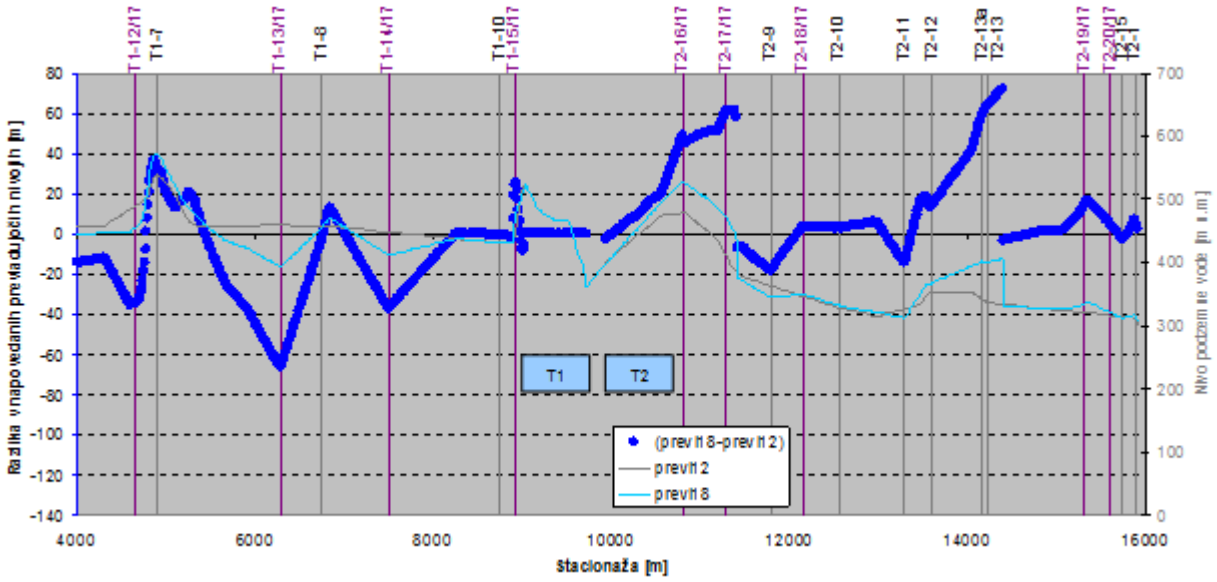

Figure 7: Difference in prediction of dominant groundwater levels in the basic design (PGD, 2012) and execution design (PZI, 2019) phases

With such two-phase borehole sets, we can conclude that both forecasts of the highest groundwater levels, only roughly, follow similar dynamics along with the levels of both tunnels. However, significant local discrepancies occur between the two forecasts: these in the T1 tunnel are mainly reflected in significant local reductions in the measured groundwater levels (T1-12/17, T1-13/17, and T1-14/17) compared to the previously forecast at both maximum and dominant groundwater levels.

In the flysch rocks area (lower part T1 and upper part T2), both the highest and the dominant levels show higher than previously predicted. Due to the low permeability of flysch rocks, such an increase does not have a significant influence on the definition of water inrush to the tunnel, nor on the choice of the tunnel implementation method (drained, undrained), but indicates the difficulty of interpolating the levels over long distances.

In the rest of the T2 tunnel, groundwater levels are much higher than initially predicted, especially in the thrust area, especially at the Socerb thrust fault. The conditions of T2-13, T2-13a boreholes (drilled in 2013) led to monitoring in 2017. The boreholes are less than 100 m apart from the tunnel route, the difference in the highest levels between them; it is as much as 50 m. More than on any section of the route of the two tunnels, the heterogeneity of the permeability field and the dependence of the groundwater level on the local conditions of supply and runoff are evident here. A similar situation can probably be expected in the karst zones along the Kastel and the Škrklovica thrust fault.

For this reason, it is necessary to take into consideration estimated piezometric groundwater levels, along with the tunnel route T1 to T2 between individual measure sites, as possible rough values. The perceived variability of piezometric pressures at sites indicates that it is probably only part of the complexity of the karst system available to be calculated in the design of all tunnels.

5.4 Layer permeability

The table below presents the essential statistical characteristics of the permeability of individual lithologic sections in the tunnel area T1 and T2 (mean and standard deviation), with statistics provided separately for the research phase (Table 1).

Table 1. Main permeability statistics by individual lithological sections (total and separately by year)

Geological structure	Year of measures	K_{middle} [m/s]	$K_{middle+std}$ [m/s]	Remark	Porosity [%]	Corec. factor
ANA/E	2011	1,0E-06	1,0E-05		0,30	1,1
	2018 water pouring test	4,3E-07	5,2E-06			
	2018 used	5,3E-07	7,5E-06	Iz T2		
F/E	2011	6,0E-07	1,0E-06		0,10	1,15
	2018 water pouring test	5,0E-08	7,2E-07			
	2018 used	5,0E-08	1,0E-06	Iz T2		
PP/E	2011	1,0E-07	3,0E-07		0,10	1,2
	2018 water pouring test	7,8E-08	1,0E-06			
	2018 used	1,1E-06	1,3E-06	Iz T1		

The default representative values for each lithology were assumed calculations of mean values, taking into account the standard deviation. These values represent the upper limit values that can be obtained by various calculations and interpretations. However, in the area of higher karst activities (e.g., near tectonic zones), much higher permeability can be expected (Table 2).

Table 2. Permeability values used after preliminary investigations

Geological structure	Year of measures	K [m/s]	Porosity [%]	Corec. factor
Fault/cavern	2011	3,01E-03		1,1
Fault zone, flysch, Lower Trstelj layers	2011	4,81E-06		1,1

5.5 Estimation of water inrush during excavation after RMR

By calculating the inflow estimate every 25 m, we were able to classify sections into 4 RMR classes according to the estimated inflow volume (l/min/25 m). In doing so, we have taken into account the inflows calculated concerning the short-term inflow and the current groundwater level.

Table 3. RMR permeability classification

No.	General conditions	Pw l/min/10m	l/s/10m
1.	Dry to moist	0 to 10	0 to 0,17 l/s
2.	Wet	10 to 25	0,17 to 0,42 l/s
3.	Leaking	25 to 125	0,42 to 2,1 l/s
4.	Water flow	>125	More than 2,1 l/s

Due to the characteristic variable permeability and the occurrence of tectonic zones, relief will only occur at the point of penetration through the tectonic or more permeable zone. In these cases, more significant point water inrushes in the form of leakage or water flow can be expected. It should be noted that in some places,

hydrogeological conditions in case of occurrence of caverns or karst caves filled with water may be significantly worse. Caverns filled with water can also be expected to have higher inflows of water.

Point inflows in such zones could, according to rough estimates, infiltrate hundreds of litres per second of flow, but would decrease significantly over time (order of 10 days magnitude) due to the emptying of porous parts of geological layers, depending on the size of »the reserves«. It should be noted that water intrusions in the area of the karst channels can exceed the derived estimate since they were taken into account in the calculations as homogenized tens of meters wide bandwidth of 10^{-3} m/s. These parts are specially marked on the longitudinal profile in Annex G.2.

5.6 Probability of water intrusion locations along with the karst channels

Monitoring up to date, combined with complementary investigations, provides a more certain interpretation of the connection between structural geological elements and the occurrence of fissure systems and karst caverns. The exact position of the karst channels cannot be predicted, but it is possible to highlight the conditions that increase the likelihood of such a phenomenon:

a. more substantial inflows or intrusions of water through the karst channels can also occur in the unsaturated zone, but only during increased infiltration and subsequent leakage;

b. in the saturated zone, intrusions may occur after the transition of the tunnel face from the massive limestone to the cracked or karst one, which is most likely to cross the fault zones or karst cracks, especially between differently permeable parts of layers;

c. water intrusions or increased water inrushes are also more likely to occur in zones of increased infiltration in areas of karst fields, or dry karst valleys and flysch and carbonate layer contacts.

Based on the above findings, the areas of the probability of water intrusion through the karst channels were classified into four classes (small, medium, higher and maximum probabilities), which are presented in the longitudinal section of Annex G.2.

The areas of the highest probability of water intrusion through the karst channels were predicted on the sections where, at the height of the level, the fault zones (the forecast geological profile), and the caverns or caves filled with water are expected. Due to the fault zones and the width of these zones, the areas of maximum probability of water intrusion along the karst channels were extended 50 m to each side of the predicted chainage of occurrence.

5.7 Technical design of the tunnel drained / undrained in bypasses

The drained sections of the tunnel are foreseen for those sections where lower permeability and fewer fissure systems and decreased karst have been determined, that is, especially in flysch layers (F/E) and the Transitional layers (PP/E). The sections of tunnels T1 and T2 where the tunnel is executed drained or undrained are shown in the longitudinal section of Annex G.2.

In areas where the tunnel tube will intersect and partially or completely cover the existing groundwater conductor (cavern, tunnel, cave), bypass, groundwater will be provided. The main purpose of the circulation is to ensure a smooth flow of groundwater through the existing conductive structures, thus ensuring:

- water conservation aspect, that is, maintaining the groundwater flow regime; and

- geotechnical aspect, preventing the seepage of vertically infiltrated water and creating further elevated hydrostatic pressures in the karst aquifer with low levels of highly localized porosity.

Due to the appearance of conductive structures of different sizes and the direction of extension, the cross-sections of these structures with a tunnel tube may comprise a relatively broad range of possible values that will dictate the

size of the required circulations. Their sizing should also take into account the magnitude of the maximum flows through the conductor, as borehole as the location of the discharger (saturated, unsaturated zone) and the presence of accompanying cracks or other small associated voids in the immediate vicinity, which could partially assume the role of circulation.

In the T1 tunnel area, we identified thirteen such sections and five such sections in the T2 tunnel area where groundwater circulation may be required. These sections are defined as the sections with the highest probability of groundwater intrusion through the karst channels. In each such section, we anticipate the need to make circulations by providing at least the same cross-section as the intersected natural karst channel. In doing so, it is recommended that at least a certain number of type bypasses be predicted, given the typical dimensions of the occurrence of the karst channels.

It should be emphasized that the occurrence of the karst channels is not exclusively related to secure fissure zones, but may also develop in the case of weak cracks. As a result, the tunnel may also encounter the karst channel on intermediate, possibly drained sections. In this case, too, a bypass should be carried out if the tunnel closes the karst channel with a continuous or intermittent flow of groundwater.

5.8 Estimation of total water inrush from the tunnel after construction

We divide water inrush to the tunnel in:

- **Short-term water inrush,** which is related to the maximum inflow of water in a developed depression funnel,
- **Long-term water inrush**, which is related to developed depression funnel and is limited in the long term by the total amount of rainfall supply.

The results are summarized in the tables below.

Table 4. Estimated water inrush to the tunnel during construction and operation for different values of permeability coefficient and groundwater levels for tunnel T1

Water inrush to the tunnel	Calculated inflow into the K_{middle} tunnel (l/s) at the dominant - maximum groundwater level	Calculated inflow into the K_{middle} tunnel (l/s) at the dominant - maximum groundwater level
Short-term water inrush (maximum inflow at depressed funnel)	106-133	56-69
Long-term water inrush (equal to the power supply in the tunnel impact area)	17-21	11-13

Table 5. Estimated water inrush to the tunnel during construction and operation for different values of permeability coefficient and groundwater levels for tunnel T2

Water inrush to the tunnel	Calculated inflow into the K_{middle} tunnel (l/s) at the dominant - maximum groundwater level	Calculated inflow into the K_{middle} tunnel (l/s) at the dominant - maximum groundwater level
Short-term water inrush (maximum inflow at depressed funnel)	66 – 78	180 – 218
Long-term water inrush (equal to the power supply in the tunnel impact area)	11 – 12	24 – 29

It is estimated that, if the tunnel were completely drained, the quantities would be about 3x higher.

5.8.1 Implementation of seepage of drained groundwater in the area of the water protection area Rižana

For the planned drained and undrained sections of T1 and T2 tunnels, a certain amount of groundwater will collect along the level fall of the tunnels, which will drain permanently outside the tunnel and aquifer. Considering the hydrogeological conditions and sinking abilities, which will only be conclusively, defined when the tunnel tubes are opened, it is necessary to look for the possibility of sinking the collected back groundwater through a system of non-return trapdoors. The purpose of the measures is to retain as much groundwater as possible in the aquifer before out-flowing the T2 tunnel. Depending on the sinking abilities on the south side of the T2 tunnel, the distribution of undrained sections in the northern side of the T2 tunnel can be optimized, in particular, in the tunnel T1, from which the drained water must be infiltrated to T2. Given the known lack of groundwater, it is unwise to discharge the latter into surface watercourses permanently.

In case of sinking, special attention should be paid to ensuring the separation of the backwater from the waters from the tunnel itself, which are in contact with the interior of the tunnel, the railway line, the consequence of washing the tunnel, etc. In order to ensure the adequacy of the sinking water, a risk analysis for the groundwater contamination of the Rižana water source must be updated when drafting the project documentation and sinking detail.

5.8.2 Deposition of flowstone in the drainage pipes

The process of the flowstone sedimentation from groundwater flowing into the drainage pipes is due to the loss of calcium carbonate from the solution in areas of increasing pH or contact with air, eliminating excess CO_2. Groundwater flowing into the tunnel will previously flow through covered and cracked limestone or flysch rocks. In both cases, the water before it drains into the drainage pipes carries with its concentrations of minerals that it cannot retain after the CO_2 excess is released.

Thus, for drainage pipes with open-air access, excretion that is more frequent is possible within:

- contact between the saturated zone of the porous medium (aquifer, reservoir) and the drainage pipe slots,
- "jumps" in the longitudinal profile of the discharge pipes,
- pipes which do not have a smooth surface,
- constrictions, knees, valves, etc.

Increasing deposit of flowstone represents a decrease in the drainage capacity of the system and a delay in hydrostatic pressures. The seepage water can also affect other parts of the tunnel, especially if the waterproofing is interrupted, where, when dried and precipitated for the lining; stresses can form on the formation of salt crystals, which can lead to the local decomposition of the concrete lining. Maintaining drainage function is, therefore, essential for the integrity of tunnel elements, which is associated with high maintenance costs.

In order to minimize the loss of minerals in the drainage pipes themselves, it is necessary to look for solutions in the direction of reducing the contact surface with air. An example is a pressure line system with siphons and overflows in which the pipe is filled with water. In this case, flowstone occurs mainly on the outlet, where it can also be easily cleaned or easily replaced. Any measures that increase the surface area, on which the drained water can interact with the air, will aggravate the state of flowstone deposits.

To reduce flowstone depositing it is reasonable to design the system in the following ways: (1) it has as few "jumps" as possible, (2) flow is laminar (low gradients), (3) the pipes are not too large but still large enough to be cleaned inside, (4) smooth enough, and (5) in case artificial materials are used they must not be laminated.

6 GEOLOGICAL-GEOMECHANICAL CONDITIONS

6.1 Typical Engineering Geological (GT) Units

We have included similar geological materials in the typical engineering-geological (GT = ground type) units, in which we expect similar behavior and are determined mainly based on lithology, taking into account the cracks and weathering (rocks and surface discontinuities) recorded on the outcrops and boreholes. In total, we determined 2 GT units describing the soil (GT0a), respectively transition to weathered rock on flysch (GT0b), 8 GT units describing the rocks (GT1a, 1b, 2a, 2b, 3a, 3b, 4a, 4b).

The last two units describe tectonically jointed rocks, namely in limestones and sandstones (GI5a), where tectonic breccia occurs (larger grains to blocks), and in marlstones (GT5b), where tectonic crumbs occur (fine-grained to fine material). The key figures for each unit are summarized in the table below.

Table 6. Typical GT units with key EG data

GT	Description	Level of tectonical damage	Crack distance (mm)					Shape of discontinutiy				Rock strength (MPa)							GSI	RQD (on the base of boreholes)
								roughness		shape										
			200-600	60-200	20-60	6-20	<6	rough	tectonically smooth	cascading	flat	R0 (0,25-1)	R1 (1-5)	R2 (5-25)	R3 (25-50)	R4 (50-100)	R5(100-250)	R6 (> 250)		
0a	Surface rock	N/A	N/A					N/A				N/A							N/A	N/A
0b	Heavily weathered rock	N/A	N / A					N / A				N / A							< 25	< 25
1a	Flysch: mainly sandstone (possible thick layers of calcarenit) (L : P = >70% : <30%)	low	X	X				X		X	X				X	X	X		50-70	tipically > 50 % often > 75 %
1b		middle to high		X	X	X		X	X	X	X			X	X	X			35-50	tipically > 50 % often > 25 %
2a	Flysch: sandstone and marlstone in similar quantities (L : P = ~50% : ~50%)	low	X	X				X		X	X			X	X	X			40-55	tipically > 50 % often > 75 %
2b		middle to high		X	X	X		X	X	X	X			X	X				25-40	tipically > 50 % often > 25 %
3a	Flysch: mainly marlstone (L : P = >70% : <30%)	low	X	X				X		X	X			X	X	X			35-45	tipically > 50 % often > 75 %
3b		middle to high		X	X	X		X	X	X	X		X	X	X				25-35	tipically > 50 % often > 25 %
4a	limestone, dolomite	low	X					X		X	X			X	X	X			60-90	tipically > 50 % often > 75 %
4b	limestone, dolomite (jointed)	middle to high		X				X		X					X	X			45-60	tipically > 50 % often > 25 %
5a	Heavily tectonized material; folded, fractured. Mainly fractured deformations, in GT units EG1a, 1b 4a and 4b	high to very high				X	X	X	X	X			X	X	X				15-30	< 20
5b	Heavily tectonized material; folded, fractured. Mainly ductile deformations, in GT units EG2a, 2b, 2a and 3b	high to very high				X	X		X		X		X	X					10-20	< 20

The distribution of individual GT units along tunnels is given in the longitudinal section in Annex G.2, and the appearance of individual GT units as recorded in the boreholes is shown in the next section.

6.1.1 Characteristic representations of selected rock mass types (GT)

The eight rock mass types selected were determined based on the mapping of outcrops, boreholes, and the results of field and lab tests. Rock mass types combine typical lithological units, comparable in mechanical and structural parameters, into classes. An estimate of their occurrence along the tunnel excavation area is shown in the longitudinal section of Annex G.2.

Highly weathered and decayed rock mass passes into the soil and strongly weathered rock mass. Here structure is still visible, and that is why it has been classified in the rock mass type GT0. Type 0a is occurring also in the form of residual clays on limestone surface and in flysch rocks weathered to clay and sand. On the other hand, cuts and sections of weathered rock with preserved structure appear in type 0b.

0a (borehole T1-5 (0-3 m)) **0b** (borehole T2-19 (0-3m))

Figure 8: Representation of characteristic borehole cores of type 0a and 0b

There are two distinctly different geological units along the tunnel route - carbonate rocks and clastic flysch rocks. The unit of carbonate rocks combines limestones and dolomites occurring along the route (GT4). The unit of clastic flysch rocks, however, is divided into three independent units, according to the ratio of sandstone and marlstone content. Analysis of the boreholes' and outcrops' descriptions of the rock mass have revealed that we can expect sections where mostly sandstone occurs (GT1), sections where sandstone and marlstone occur in roughly similar proportions (GT2) and sections dominated by marlstone (GT3).

The dominant sandstone deposits (P: L => 70%: <30%) usually have a thick layering with thin intermediate layers of marlstone. Thicker layers of thick-grained calcarenite sandstone are also possible. Tectonically intact dominant sandstones form compact sections whose stalls are conditioned by discontinuities (1a), whereas areas with a higher degree of fissure systems (1b) are present in tectonically slightly to moderately faulted areas.

1a (borehole T2-21 (18-22m)) **1b** (borehole T2-19 (8-12 m))

Figure 9: Representation of characteristic borehole cores of rock mass type GT1a and GT1b

The sections where approximately the same sandstone-marlstone ratio occurs (P: L = 50%: 50%) are characterized by thinner layering (ranging from several cms to dm), where marlstone and sandstone layers alternate. The weak component in the package is represented by layers of marlstone, which, upon contact with atmospheric conditions or water, decompose (2a), and in the area of significant tectonic damage, assume most of the deformations and form more cracked and shear-deformed sections with transitions in earth-like materials (2b).

2a (borehole T1-15/17 (195-200 m)) **2b** (borehole T2-7 (110-115 m))

Figure 10: Representation of characteristic borehole cores of rock mass type GT2a and GT2b

The predominant marlstone compositions (P: L => 30%: <70%) are typically thinner layered (usually up to several cms), with lower strength. This unit also includes pure marlstones of the area, i.e., transition layers. In tectonically less fractured sections, they can act massively (3a) but, when exposed to atmospheric conditions or water, are prone to rapid weathering and decay. Tectonically fractured sections are characterized by fissured areas with visible shear deFormations and transitions in earth-like materials (3b).

3a (borehole T1-11 (76-81 m)) **3b** (borehole T2-1 (46-51 m)

Figure 11: Representation of characteristic borehole cores of the rock mass type GT3a and GT3b

The carbonate areas are composed of limestones and dolomites. The thickness of the layering can be very different, from a few inches to a massive rock. Tectonically entire sections represent compact and homogeneous areas (4a), while for tectonically fractured areas, more fissured sections may appear, as borehole as more clayed sections than crack fillings (4b). Particularly in thin-film and cracked areas, an increased occurrence of karst structures, which may be in the form of different cavities and tunnels, which may be empty or filled with sediment or water, can be expected.

4a T2-12 (48-54 m) **4b** (vrtina T1-8 (110-116 m))

Figure 12: Representation of characteristic borehole cores of the rock mass type GT4a and GT4b

Within the rock mass units, there are areas of fractures where the rock is damaged and deformed. Such areas are generally up to one meter thick and are counted as units under code b (1b, 2b, 3b, and 4b). Larger zones occur

mainly in thicknesses up to 5 m, but rarely more (5a and 5b). In these zones, there has been deformation of the bedrock, so it exhibits different characteristics than the base unit. Depending on the stiffness of the rock, the shape and location of the deformation, they are divided into:

- areas dominated by fracture deformations - mainly related to the outer fracture zones and areas of more rigid rocks (limestones, dolomites, and sandstones). The rock occurs in the form of blocks, tectonic breccia, and fault gouge (Unit 5a);
- areas dominated by ductile deformations - mainly related to internal fracture zones and areas of fine-grained clastic rocks (marlstones). The ridge is sanded, wrinkled, and curved and can also wholly decompose in soil-like materials (Unit 5b).

The characteristic appearance of the rock unit is shown in Figure 13.

5a (borehole T2-13 (36-39 m))

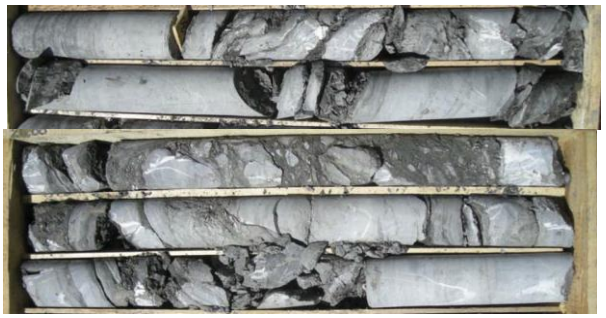

5b (borehole T1-11 (23-29 m))

5a (vrtina T2-20/17 (60-95 m))

5b (borehole T1-15/17 (145-150 m))

Figure 13: Representation of characteristic boreholes cores of the rock mass type GT5a and GT5b

The typical appearance of individual types of rock units is shown in Figures 8 to 13.

6.2 Geomechanical parameters of individual GT units

The geomechanical parameters of individual rock mass GT units were determined based on a statistical analysis of all field and lab tests performed. For parameters where few data was obtained from field and lab tests, the parameters were estimated based on experience with similar materials and recommendations from the literature. The parameters are specified for both soil and rock.

The individual geomechanical parameters were determined and are presented from 1 to 15 in the list below.

(1) Values determined based on lab tests and on experiences with similar materials.

(2) Value determined based on analysis of lab tests (3rd and 1st quartile); for GT5a and GT5b, the default minimum lab values are measured for limestone (TG4) and marl (GT3).

(3) Characteristic values (at 95% confidence) based on lab analysis; for GT5a the characteristic values for sandstone are assumed as the lower of the two values of the materials from which GT (GT5a) and for (GT5b) are derived, and the value for marlstone is assumed.

(4) Values based on the analysis of boreholes.

(5) Values determined from boreholes and recommendations of Marinos et al. (2007).

(6) Values based on literature recommendations.

(7) Value based on analysis of lab tests (3^{rd} and 1^{st} quartile); for GT5a and GT5b, due to an insufficient number of samples, values cannot be determined.

(8) Recommended values for the 3^{rd} quartile of lab test analysis, except for GT2a, b where, due to the influence of sandstone, the 3^{rd} quartile is not the default but the median; for GT5a and GT5b, E_i defaults to GT1a and GT3a respectively.

(9) Values based on literature recommendations, where mechanical excavation will take place, D=0 is considered, where mining is envisaged, D=0.2 is considered in the range of the first 0.5 to 1.0 m of the hill.

(10) The GT0a and GT0b values based on feedback analyse, and lab data are calculated for the other GTs according to the HB criterion.

(11) Minimum and maximum E_{rm} values were based on HB calculation.

(12) The dominant lithology on the section based on the census of boreholes and the structural-geological model.

(13) Characteristic value (at 95% and 90% confidence, respectively) of the load loop based on field pressiometer tests.

(14) Characteristic value (at 95% and 90% confidence, respectively) of the release-load loop based on field pressiometer tests.

(15) The values for GT0a and GT0b and GT5a and GT5b are based on the literature, the other values being typical values of the results of lab tests.

In addition to the geomechanical parameters of the individual GT units, we also give the estimated values of the shear characteristics of the discontinuities that occur in the individual units.

The results of the field and lab tests are presented in detail in Annex P.2.

Table 7. Geomechanical parameters for characteristic engineering-geological units (GT) and discontinuities in single units

	γ	σ_c		RQD	GSI	before	Ed	Ei	D	c'		φ'	E_{rm}	dominant lithology in the section	E1	E2	ν
	(kN/m³)	(MPa)					(MPa)	(MPa)		kPa			(MPa)		(MPa)	(MPa)	(-)
	suggested	lab	σci charact.		suggested		lab	suggested	suggested				min-max		charact.	charact.	charact.
	(1)	(2)	(3)	(4)	(5)		(7)	(8)	(9)	(10)			(11)	(12)	(13)	(14)	(15)
0a	19	-	-	na	na		-	-	-	2			-	cl, clgr	-	-	0,30
0b	23	-	-	<25	<15		-	-	-	10			-	totaly weathered rock	109	249	0,25
1a	26	122	62	tipically > 50 % often > 75 %	50-70	45-65	39823	39823	0,2	calculation by HB		34	9209 - 24233	Flysch: mainly sandstone (possible thick layers of calcarenit) (L : P = >70% : <30%)	20127	28105	0,20
1b	26	56		tipically > 50 % often > 25 %	35-50		14377					28	3403 - 9209		5702	11634	
2a	26	46	36	tipically > 50 % often > 75 %	40-55	35-45	34800	21387	0,2 (0,0) depends of the excavation technology			28	2544 - 6698	Flysch: sandstone and marlstone in similar quantities (L : P = ~50% : ~50%)	8377	14814	0,23
2b	26	39		tipically > 50 % often > 25 %	25-40		10150					25	1280 - 3414		3843	4451	
3a	26	31	15	tipically > 50 % often > 75 %	35-45	30-45	15579	15579	0,0			24	1766 - 3484	Flysch and transitional layers: mainly marlstone (L : P = >70% : <30%)	3935	6285	0,26
3b	26	15		tipically > 50 % often > 25 %	25-35		6016					21	932 - 1766		2448	6640	
4a	26	74	64	tipically > 50 % often > 75 %	60-90		47871	47871	0,2			36	19579 - 40633	limestone, dolomite	25245	32590	0,18
4b	26	35		tipically > 50 % often > 25 %	45-60		17833					29	7978 - 19579		7133	19191	
5a	26	9	62	<20	15-30		-	39823	0,2			23	1250 - 2496	*please see* ** *below the table*	2058 (min 1090)	5068 (min 4422)	0,22
5b	26	5	15	<20	10-20		-	15579	0,0			17	475 - 711		2314 (min 1742)	7934 (min 5291)	0,25

GT	Discontinuity type	ϕ (°)	c (MPa)
1	Layer (SS), crack (J)	25-30	0
2	Layer (SS), crack (J)	20-30	0
3	Layer (SS), crack (J)	15-25	0
4	Layer (SS), crack (J)	30-35	0

* *	Heavily tectonized material; 5a <- block material (mainly fractured deformations) 5b <- finegrained material (mainly ductile deformations)

6.3 Geological-geomechanical conditions along the route

The geological-geomechanical conditions along with the route of T1 and T2 tunnels are described in detail in references [2] and [3] and presented in the longitudinal sections in Annex G.2. The schedule of typical GTs is summarized in the table below.

Table 8. Geological-geomechanical conditions along with T1 and T2 tunnels

	Chainage		Length	GT (%)												Bid angle	block's fallout	Pre. Zone
	from	to		0a	0b	1a	1b	2a	2b	3a	3b	4a	4b	5a	5b			
1	2979	3100	121		20%							###	60%			C	Med.	
2	3100	3271	171		8%							###	67%			C	Med.	
3	3271	3291	20		10%								10%	80%		C	Maj.	Yes
4	3291	3400	109		8%							###	67%			C	Med.	
5	3400	3420	20		10%								10%	80%		C	Maj.	Yes
6	3420	4252	832		5%							###	60%			C	Med.	
7	4252	4277	25		10%								10%	80%		C	Maj.	Yes
8	4277	4647	370		5%							###	80%			C	Med.	
9	4647	4710	63		10%								40%	50%		C	Med.	Yes
10	4710	4820	110									###	55%	5%		C	Med.	
11	4820	4845	25		10%								10%	80%		C	Maj.	Yes
12	4845	5643	798		5%							###	50%			C	Med.	
13	5643	5668	25		10%								10%	80%		C	Maj.	Yes
14	5668	5996	328		5%							###	50%			C	Min.	
15	5996	6226	230		5%							###	65%	5%		C	Min.	
16	6226	6320	94		75%								20%	5%		C	Min.	
17	6320	6494	174		5%							###	55%	5%		C	Min.	
18	6494	7064	570		5%							###	55%			U	Med.	
19	7064	7089	25		10%								10%	80%		U	Maj.	Yes
20	7089	7296	207									###	70%	5%		U	Med.	
21	7296	7322	26		10%								10%	80%		U	Maj.	Yes
22	7322	8036	714									###	60%	15%		U	Med.	
23	8036	8287	251		5%							###	65%	5%		U	Med.	
24	8287	8312	25		10%								10%	80%		U	Maj.	Yes
25	8312	8430	118		5%							###	65%	5%		U	Maj.	
26	8430	8455	25		10%								10%	80%		U	Maj.	Yes
27	8455	8483	28									###	80%	5%		U	Maj.	
28	8483	8508	25		10%								10%	80%		U	Maj.	Yes
29	8508	8853	345		5%							###	60%	5%		U	Maj.	
30	8853	8939	86					20%	40%		20%			5%	15%	C	Maj.	Yes
31	8939	9427	488			###		20%	20%	###	15%				5%	C	Med.	
32	9427	9623	196			###	###	20%	20%						10%	C	Maj.	
33	9623	9679	56	5%	10%	###	###		40%						5%	C	Med.	
				T2														
1	9928	10046	118	5%	10%		###	20%	5%	###						U	Med.	
2	10046	10284	238			###	###		30%						5%	U	Med.	
3	10284	11063	779			###	###	8%	7%						5%	U	Med.	
4	11063	11295	232							###	30%				5%	U	Maj.	
5	11295	12500	1205	2%								###	33%	5%		U	Maj.	
6	12500	12594	94	5%								###	55%	10%		U	Maj.	Yes
7	12594	13400	806	2%								###	28%	5%		U	Min.	
8	13400	13510	110	5%									85%	10%		U	Maj.	Yes
9	13510	14000	490	2%								###	23%	5%		C	Med.	
10	14000	14140	140	5%							45%		15%	10%	25%	C	Maj.	Yes
11	14140	14240	100							###	45%				5%	C	Med.	
12	14240	14884	644	2%								###	23%		5%	C	Maj.	
13	14884	15122	238	5%								###	60%	5%		C	Maj.	
14	15122	15238	116	2%							52%		18%	10%	18%	C	Maj.	Yes
15	15238	15634	396							###	60%				20%	C, U	Maj.	Yes
16	15634	15802	168	2%							43%		10%	15%	30%	U	Maj.	Yes
17	15802	15930	128	2%							58%				40%	C	Maj.	Yes

C (convinient) U (unconvinient), depends on tunnel face forward motion direction

Maj. (major), Med. (medium), Min. (minor)

7 GEOLOGICAL-GEOTECHNICAL BASE OF DESIGN

7.1 General

From a design point of view, it is necessary to provide the geological-geotechnical bases for the design of tunnels and portals and accompanying objects on portals (engine rooms, fan stations, etc.). The parameters given in the previous section allow the designer to perform the necessary strength-deformation analyses based on which he can determine the necessary support measures. Below we summarize the critical orientations that will help the designer and guide.

7.2 Tunnel excavation

7.2.1 Deformation potential

The tables below give the estimated deformation potential by the Hoek method [9], which is otherwise predicted for more extensive diameter tunnels and is conservative from this point of view. On the other hand, it assumes an isotropic homogeneous medium and therefore does not take into account the anisotropy in deformation properties, the influence of discontinuities, anisotropy of the stress field, etc., so it is of a more orientation character. We tested two voltage assumptions, namely that the horizontal and vertical stresses are the same, and that the horizontal is 1.5x higher - similar values were found by hydrofracturization in the area of tunnel T8 - Lot 2.

Table 9. Deformation potential in individual GT units by depth

			Depth										
			5	10	20	30	50	100	150	200	250	300	350
			In situ stress σv=σh										
		σcm (MPa)	0,125	0,25	0,5	0,75	1,25	2,5	3,75	5	6,25	7,5	8,75
GT (deformation potential)	1a	11	88	44	22	14,67	8,8	4,4	2,93	2,2	1,76	1,47	1,26
	1b	7,6	60,8	30,4	15,2	10,13	6,08	3,04	2,03	1,52	1,22	1,01	0,87
	2a	4,4	35,2	17,6	8,8	5,87	3,52	1,76	1,17	0,88	0,7	0,59	0,5
	2b	2,9	23,2	11,6	5,8	3,87	2,32	1,16	0,77	0,58	0,46	0,39	0,33
	3a	1,5	12	6	3	2	1,2	0,6	0,4	0,3	0,24	0,2	0,17
	3b	1,1	8,8	4,4	2,2	1,47	0,88	0,44	0,29	0,22	0,18	0,15	0,13
	4a	12,7	101,6	50,8	25,4	16,93	10,16	5,08	3,39	2,54	2,03	1,69	1,45
	4b	8,9	71,2	35,6	17,8	11,87	7,12	3,56	2,37	1,78	1,42	1,19	1,02
	5a	3,4	27,2	13,6	6,8	4,53	2,72	1,36	0,91	0,68	0,54	0,45	0,39
	5b	0,64	5,12	2,56	1,28	0,85	0,51	0,26	0,17	0,13	0,1	0,09	0,07
			Globina										
			5	10	20	30	50	100	150	200	250	300	350
			In situ stress σvx1.5=σh										
		σcm (MPa)	0,17	0,33	0,67	1	1,66	3,33	4,99	6,65	8,31	9,98	11,64
GT (deformation potencial)	1a	11	64,71	33,33	16,42	11	6,63	3,3	2,2	1,65	1,32	1,1	0,95
	1b	7,6	44,71	23,03	11,34	7,6	4,58	2,28	1,52	1,14	0,91	0,76	0,65
	2a	4,4	25,88	13,33	6,57	4,4	2,65	1,32	0,88	0,66	0,53	0,44	0,38
	2b	2,9	17,06	8,79	4,33	2,9	1,75	0,87	0,58	0,44	0,35	0,29	0,25
	3a	1,5	8,82	4,55	2,24	1,5	0,9	0,45	0,3	0,23	0,18	0,15	0,13
	3b	1,1	6,47	3,33	1,64	1,1	0,66	0,33	0,22	0,17	0,13	0,11	0,09
	4a	12,7	74,71	38,48	18,96	12,7	7,65	3,81	2,55	1,91	1,53	1,27	1,09
	4b	8,9	52,35	26,97	13,28	8,9	5,36	2,67	1,78	1,34	1,07	0,89	0,76
	5a	3,4	20	10,3	5,07	3,4	2,05	1,02	0,68	0,51	0,41	0,34	0,29
	5b	0,64	3,76	1,94	0,96	0,64	0,39	0,19	0,13	0,1	0,08	0,06	0,05

Areas, where numbers are written in pink, they do not show within the tunnel route

0-0,17	Very high deformation potencial - at the limit of feasibility
0,18-0,3	High deformation potencial
0,3-0,5	Moderate deformation potencial
>0,5	Standard conditions

As can be seen from the table above, a very high deformation potential can be expected in GT3b units at depths of 200 m (only in the Socerb fault thrust in T2 tunnels), and in G5b units at depths above 150 m (areas of fault lines and contacts mainly in the tunnel T2). High deformation potential can be expected in GT3a, 3bm 5a and 5b units at depths above 100 m (in both tunnels), and moderate or negligible in all other cases.

7.2.2 Determination of geotechnical behaviour of rock mass (BT) and the distribution of behavior types

For design, it is necessary to determine the specific geotechnical types of rock mass behavior (BT) that describe the expected behavior of an unsupported rock mass under specific geotechnical conditions. These conditions depend on the engineering-geological units (GT), their properties, and indirect factors such as the presence of water, primary in-situ voltage, the orientation of the discontinuities, and the dimensions and shape of the excavation. As can be seen from the table below, based on the analysis of available results, we have identified six (out of eleven) basic types of behavior in the tunnel area, which in our opinion describe the excavation conditions of tunnels T1 and T2.

Table 10. Characteristic geotechnical types (BT) of rock mass behaviour

Behaviour type (BT)		Description of mechanisem's modes of potencial failures generated during the excavation of unsupported rockmass	Occurence in GT units
1	Stable	Stable rrockmass with potential of local gravity failures, defining blocks possible to fall or slide.	Dominant: 1a, 4a Subordinated: 2a, 3a
2	Stable with the possibility of block formation within discontinuity	Gravity fallouts and block slides conditioned by deep reaching cracks. Occasionally also shear failure.	Dominant: 1a, 2a, 3a, 4a, 4b Subordinated: 1b, 2b, 3b
3	Shallow shear failure	Shallow shear failure generated due to the load in combination with the gravity and discontinuity conditioned failure.	Dominant: 1b,2b,3b,4b Subordinated: 5a
4	Deep shear failure	Deep shear failures and large deformations generated due to loads.	Dominant: 5a, 5b Subordinated: 2b, 3b
5	Rock burst	Sudden failure caused by high overloaded brittle rocks and sudden release of accumulated stress.	
6	Failure due to layer buckling	Buckling of thinlayered rockmass plates limited by a dense system of cracks. Often together with shear failure.	
7	Shear failure beneath low stresses	Posibbility for failures of larger volumes and progressive shear failures. Normally caused by low horizontal stress and lack of layer continuity.	Dominant: 0a, 0b Subordinated: /
8	Ravelling	Ravelling of cohesionless dry or moist, severly fractured rocks.	Dominant: / Subordinated: 0b, 3b, 5a, 5b
9	Flowing rockmass/ soil	Flow of intensenly fractured rockmass or soil. Material has a high water content.	
10	Swelling	Time dependent volume increase of rockmass as a consequence of the phyisical-chemical reaction between rockmass, water and stress relief. It causes block, tunnel crown and bottom motion into the excavation space.	
11	Very heterogenous rockmass with frequently changing deformationa characteristics	A large variation of stresses and deformations conditioned by block-matrix structure (for example heterogenous disorder zones, tectonic mixture)	

A detailed description of the geotechnical types (BT) of the behavior along the route of tunnels T1 and T2 is given in references [2] and [3], and their spatial distribution is given in longitudinal sections in Annex G.2 and summarized in the tables below.

Table 11. BT arrangement along the tunnels T1 and T2 alignment

T1

	Chainage		Length	BT (%)					
	from	to		1	2	3	4	7	8
1	2979	3100	121		60%	20%		20%	
2	3100	3271	171	12%	80%				8%
3	3271	3291	20			90%	5%		5%
4	3291	3400	109	12%	80%				8%
5	3400	3420	20			90%	5%		5%
6	3420	4252	832	15%	80%				5%
7	4252	4277	25			90%	5%		5%
8	4277	4647	370	15%	80%				5%
9	4647	4710	63		20%	40%	30%		10%
10	4710	4820	110	20%	65%	15%			
11	4820	4845	25			90%	5%		5%
12	4845	5643	798	25%	60%	10%			5%
13	5643	5668	25		5%	90%			5%
14	5668	5996	328	25%	60%	10%			5%
15	5996	6226	230	15%	50%	30%			5%
16	6226	6320	94		20%	50%			30%
17	6320	6494	174	20%	45%	30%			5%
18	6494	7064	570	20%	55%	20%			5%
19	7064	7089	25			90%	5%		5%
20	7089	7296	207	15%	60%	25%			
21	7296	7322	26			90%	5%		5%
22	7322	8036	714	15%	60%	25%			
23	8036	8287	251	15%	65%	15%			5%
24	8287	8312	25			90%	5%		5%
25	8312	8430	118	15%	65%	15%			5%
26	8430	8455	25			90%	5%		5%
27	8455	8483	28		70%	30%			
28	8483	8508	25			90%	5%		5%
29	8508	8853	345	20%	65%	10%			5%
30	8853	8939	86		15%	65%	20%		
31	8939	9427	488	10%	40%	45%	5%		
32	9427	9623	196	10%	40%	40%	10%		
33	9623	9679	56		20%	70%		10%	

T2

	Chainage		Length	BT (%)					
	from	to		1	2	3	4	7	8
1	9928	10046	118		50%	30%		20%	
2	10046	10284	238		30%	65%			5%
3	10284	11063	779		60%	35%			5%
4	11063	11295	232		60%	40%			
5	11295	12490	1195	45%	40%	10%			5%
6	12490	12600	110		60%	25%	10%		5%
7	12600	13390	790	45%	35%	15%			5%
8	13390	13555	165		20%	70%			10%
9	13555	14020	465	70%	25%				5%
10	14020	14140	120		10%	50%	30%		10%
11	14140	14240	100		60%	40%			
12	14240	14810	570	60%	35%				5%
13	14810	15135	325	30%	65%				5%
14	15135	15300	165		10%	60%	20%		10%
15	15300	15575	275		15%	55%	20%		10%
16	15575	15800	225		10%	60%	20%		10%
17	15800	15930	130		20%	50%		20%	10%

7.2.3 Summary of potential geotechnical problems and guidelines for tunnel excavation

In this section we summarize the key elements that the designer and contractor need to pay attention to.

Karst phenomena

In the limestone excavation area, there is a possibility of karst phenomena, i.e., caverns and other cave spaces. In the areas as mentioned above, more substantial water inrushes and spreading of soil materials that fill the karst spaces may occur.

Besides, karst spaces may make it challenging to advance excavation works (example of bridging in the area of the invert, if larger cave spaces would appear in the excavation area). It is recommended to systematically pre-drill in front of the calotte during the tunnel excavation itself and to perform geo-radar measures.

Groundwater inrush

During the construction of the tunnel, we expect water flows only in narrow fault zones or during excavation into karst caves filled with water. Because the permeability of the fault zones is good and of the caverns is very good, water inrush can reach hundreds of liters per second of flow. Throughout the tunnel, sections were marked with the degree of probability of intrusion from borehole-permeable karst zones. The risk of water intrusion must also be taken into account when crossing the contact of flysch and the Transitional layers as well as Alveolina Nummulitic limestones. **Because the exact locations of all caves and caverns cannot be accurately predicted, practically the entire length of the tunnels will require pre-drilling.**

Design of drained/undrained tunnel sections and bypasses

The designer will have to follow the instructions and guidelines for the execution of drained and undrained tunnel sections and bypasses, as given in this document and references [1], [2] and [3].

Water aggressiveness to concrete

Samples of water taken from route two are not classified in the aggressive chemical environment by the criteria of the standard, except for the sample from borehole T2-13a, which, due to aggressive CO_2 (15.40 mg/l), is classified as a small aggressiveness chemical environment (XA1).

Loss of flats/blocks of rock mass and slip of blocks

An unfavorable combination of two or more joint systems can cause the failure (gravity controlled) of the flats/blocks of the rock mass to collapse instantly and unannounced from the tunnel ceiling. The probability of failure is higher in a suitable rock mass, where excavation steps are taken in more considerable distance step, and flats/blocks may be more extensive. Reducing excavation steps and properly anchoring the tunnel ceiling is essential to reduce the risk. The areas where these phenomena may occur are shown in the longitudinal sections in Annex G.2 and references [2], [3], [4], and [5].

Crushing

Due to exposure to water or mechanical stress, marl rock can decompose into flaky rock debris, and may even decompose into clay and mud. In order to avoid the formation of the sticky mud in the tunnel invert, all water (technological and ground) must be carefully controlled and the invert adequately protected.

Swelling

However, there are no indications based on the investigations carried out which would confirm swelling. Research results in the T4 tunnel areas, which were carried out as part of the geological-geomechanical studies of the second track of the Divača-Koper railway line, the Črni Kal-Koper section, show that particular flysch layers have swelling potential. On the other hand, experiences in the construction of the Barnica, Tabor, Markovec, and Decani tunnels show that these pressures are negligible.

The presence of pyrite in the rock

The presence of pyrite in the Transitional layers and over-kneaded layers of the Črni Kal thrust zone was detected in the cores of the boreholes. It can affect the chemical properties of the water and indirectly the concrete embedded in the primary tunnel support.

In-situ stress

It should be taken into account that the area is still exposed to active tectonic pressures in the N-S or NE-SW directions, which implicitly indicates the direction of the primary horizontal in-situ stress. In this case it is generally perpendicular to the axis of the tunnel, which is favorable. The results of hydrofracturization (in the area of tunnel T8-Lot 2) show that the horizontal stress is at least 1.5x higher than the vertical stress, and the measured direction of the maximum horizontal stress is E-W, which is quite different from the regional trends. On the other hand, a sweep carried out north of Trieste, in limestone, confirms the NE-SW direction. On the other hand, the measure carried out northern of Trieste, in limestones, confirms the NE-SW direction.

Abrasiveness

Abrasiveness tests on harder rocks (sandstones and limestones) which will occur along the tunnel tube have not been performed at this stage of research. According to the GG report of the Barnica tunnel (GG report on the conditions of construction of the Barnica tunnel on the section HC Razdrto-Vipava, km 6.2-km 11.7, version »VIOLA 1«, phase PGD, IRGO Ljubljana, 2004) the CAI test was performed on two harder flysch samples, the CAI for fine-grained sandstone was 1.9 and for limestone 1.7. Based on these data and the UCS characteristic values, the CAI index for sandstone and limestone is estimated to be 2-3 (according to Figure 10 from: "EUROCK 2004& 53rd Geomechanics Colloquium. Schubert (ed.) 2004 VGE").

Terrain seismicity

According to the Slovenian pre-standard of SIST ENV 1998-1-1, which considers a 500-year earthquake return, the route area belongs to the 7th earthquake stage. According to the ground acceleration map for 475 years return period effective from 01.01.2002, the value of the earthquake acceleration Q_g is 0.125 g for the tip of the ground - solid ground. The tunnel will be made in flysch in limestone, which according to SIST ENV 1998-1-1: 2003, Table 3.1 is classified in category A.

Material integrity

Limestone of adequate granularity, occurring in more than 80% of the tunnel route, is the first-class material for the construction of manmade fills. It is also suitable for use as an aggregate for concrete, for unbound load-bearing layers, for load-bearing asphalt layers, for mortars, and as a stone for hydro-technical works and stone retaining wall. It is estimated that excavated material in flysch layers is suitable for installation in manmade fills, but without prior deposition, which would significantly impair its characteristics and not in the final layers, at most up to a height of 1 meter below the intended level of the road body, and at least 0.5 m above the groundwater area. Given that sandstones are predominant in these layers, no significant borehole pressures are expected with the moistening of the material.

7.3 Portal areas

7.3.1 Northern portal of the tunnel T1

The broader area of the portal is represented by the heavily karst plateau, with numerous sinkholes, the bottoms of which are filled by clay and gravely eluvium. Into this eluvium, also entirely, near-surface limestone is changing; however, the thickness of the eluvium varies greatly. The area is stable. The limestone is the only rock in the portal area. It is thickly layered and subjected to heavily karst activity. Smaller caves, grykes, no-ceiling caves, and deep cracks filled with clay and gravel are to be expected.

Areas filled with clay thus localized to karst areas, width 5 m maximum up to a maximum of 20 m (otherwise in the bottom of the sinkhole). The excavation slopes are, therefore, generally stable at a slope of 5:1, which was also the case for the portal wall. Due to the protection against erosion and wedging out (as well fallouts of blocks), it is proposed to replace the clay of karst forms with stone in concrete or with shotcrete during excavation and anchorage of potentially unstable surfaces: blocks and wedges. For the sake of protection against wedging out from the bank, it is suggested that the portal tube is being pulled out from the embedded slope. Excavation will be done by mining.

The type of rock mass that is expected on the portal is 4b to 4a, locally, and within karst forms, GT0a. Due to the possible occurrence of karst phenomena below the excavation level, we suggest measuring with geo-radar at the bottom excavation. The situation in the area of the central and service pipes is similar.

7.3.2 Southern portal of the tunnel T1

In the area of southern tunnel face under the clayey gravel, mostly up to a depth of 5 m, flysch (replacement of marlstone and sandstone in marlstone/sandstone ratio = 30/70) is located. It is weathered up to a depth of 5 m and in the area were dominated by marlstone also to a depth of 15 m. Underneath lies a partially compact, partly cracked flysch. The layers are heavily folded, the dip angle changes rapidly; generally, the layers are steep to sub-vertical.

The rock mass types that are expected on the portal are such that GT1b in 2b and subordinate 1a, 0a, 0b in 5b.

The rock mass properties are in geotechnical terms quite good, which, when excavating the portal areas, enables the excavation with hydraulic hammers and the excavator, partly requires the mining process. Due to the sensitivity of flysch to weathering and sliding along the discontinuities, one should envisage the safeguards (mainly depending on the dip angle, which changes a lot locally within the Glinščica area). The situation on the main and service tunnel tube is detailed.

7.3.3 Northern portal of the tunnel T2

On the surface, there is the clayey gravel to a depth of 2.5 m, followed by weathered flysch to a depth of 5.0 m, and a more in-depth, partially compact to partially cracked flysch. The layers are strongly folded, and the dip angle varies rapidly; generally, the layers are steep to sub-vertical, and the dip angle is prosperous according to the portal. The rock mass types that are expected on the portal are GT1a and 1b, and subordinate 2a, 2b, 0a, and 0b.

Geotechnical properties of the rock mass are excellent in geotechnical terms, and, given the sandstone predominance, the excavation will be mostly done with mining processes. Due to the sensitivity of flysch to weathering and sliding along the discontinuities, one should envisage the safeguards (mainly depending on the dip angle, which changes a lot locally within the Glinščica area). The situation on the main and service tunnel tube is detailed.

7.3.4 Southern portal of the tunnel T2

The rock mass types that are expected on the south portal are GT3a and 5b and subordinate 3a, 0a and 0b. Both portals are located within the Črni Kal thrust fault, where we expect challenging geotechnical conditions. As the geological and geotechnical conditions differ slightly between the two portals, we provide them separately.

Main tube portal

The portal's top heading of the main tube is located approximately 20 m in front of the Črni Kal thrust fault contact between flysch and limestone. In the area of the top heading, the top layer of clay with gravel reaches a depth of 1.5 m, underneath which there is a strongly weathered marlstone to a depth of 5.0 m. The zone of the weathered marlstone extends underneath to a depth of 9.0 m, where the non-weathered flysch layers begin. In the lower part of the excavation (lower approx. 8 m), the rock will be severely fractured and cracked. The general bedding is auspicious for the stability of the tunnel face; the layers have a slight bid angle towards the top heading. Individual cracks with a bid angle of 30-60° out of the top heading will be inconvenient and will cause local rock crushing and fallouts of marlstone beds. For the most part, the discontinuities in the rock are flat and smooth. Water inrush will occur at the eluvium contact with the flysch bedrock; in the weathered layers, the water will drain in places. We estimate that the eluvium cover is relatively stable.

The surface and eluvium waters need to be drained. Particular attention is drawn to the karst spring, located approximately 20 m behind the top heading of the portal, which is at the straightforward contact of the limestone and the flysch. The permissible gradients of temporary embankments, in individual GT units, are therefore given in the above overviews. Any steeper open excavations higher than 3 m must be adequately protected (temporary and permanent rock bolts, reinforced mesh with shotcrete, support structures). It should be noted that flysch layers are very susceptible to the atmosphere conditions, so all the embankments should be quickly concluded or adequately protected.

Portal of the service tube

The estimated height of the excavation of the top heading is 13.5 m, and in front of the top heading, it is envisaged to make a cut-and-cover section in the length of more than 19 m. The top heading of the service tube portal is approximately 50 meters away from the thrust contact between the flysch and the limestone. In the area of the top heading, the top layer of clayey gravel and clay with the gravel reaches 2.5 m deep; underneath it lays a strongly weathered marlstone to a depth of 8 m. Only a thin layer (1.0 m) of less weathered marlstone occurs below and then weathered flysch layers already appear. In these areas, narrower zones (0.5–2 m) of fractured rock may occur. The general bedding and jointing are similar to those of the main tube area. Layers bid into the slope, locally due to the inconvenient individual cracks, where marlstone sheets fall offs may occur. **We are warning against the E and NE portal slopes, where the eluvium cover is unstable and where there have been more landslides in the past. A permanent spring is also recorded in the area. An inclinometer was set up in the T2-7 borehole located in the landslide area. According to GI ZRMK, which performed measures between February and October 2010, the inclinometer is stable. During this period, no measured displacements were indicating the depth of the sliding surface.**

By draining the area above the labile part, it will be necessary to prevent water from seeping into the labile part, and to drain as much as possible the rest of the slope. The permissible gradients of temporary slopes in individual GT units are given in the overviews above. Any steeper open excavations higher than 3 m must be appropriately protected (temporary and permanent rock bolts, reinforced mesh with shotcrete, support structures). It should be noted that flysch layers are very susceptible to the atmosphere conditions, so all the embankments should be quickly concluded or adequately protected.

8 GEOTECHNICAL MONITORING GUIDELINES AND INVESTIGATIONS IN THE EXECUTION PHASE

In the frame of geotechnical measures, monitoring of characteristic profiles on the surface and in the tunnel is suggested. The monitoring area will need to be positioned in the broader area so that the influence of individual works on deformation changes can be controlled. During construction, it will be necessary to carry out geotechnical and control measures on an ongoing base in order to identify possible redistribution of stress and to control the stability of the tunnel. Geotechnical measures are used to optimize support measures, and working phases and are an integral part of the excavation technology.

We suggest performing the following minimum measures:

- underground trigonometric measures (to control the deformation of the rock mass around the tunnel tube);
- multipoint extensometers (detecting displacements and changes in stress in the surrounding rock mass around the tunnel tube, including sliding and material relaxation);
- measuring rock bolts (measuring the degree of rock bolts' mobilization and changes in tension in the rock bolts around the tunnel tube, including sliding and relaxation of the material);
- surveying and measuring changes in tension status on the surface in the area of tunnel faces;
- measures with laser scanner technology (terrain laser scanner - TLS) both before the start of construction, during tunnel construction, and after tunnel construction is completed;
- systematic geo-radar measures of the rock mass and radial measures around the tunnel and in the front of the tunnel (structural and lithological characteristics of the surrounding rock mass, advance positioning of possible karst phenomena, etc.);
- inclinometer measures in the north and south portals;
- measures of groundwater levels in piezometers (during and before construction) and in built-in measuring sites of piezometric pressures along the tunnel (during construction);
- measures of water inrush and their changes over time as each tunnel tube progresses;
- measures provided in the risk analysis measures;
- the effects of tunnel construction and operation on the quality and quantity of groundwater are monitored at the spring of the Osap River, at the sources at Boljunc and at the Rižana catchment area, where annual state monitoring of groundwater quality is already being carried out. In the flysch rock area, the impact of tunnel construction and operation is checked on the left inflow (without a name) of the Glinščica River, which is passing by the northern tunnel portal.

We suggest that from the list of measures, the following ones are executed in the phase of construction: pre-drilling into the top heading, waists, crown, and bottom, especially in parts where underground spaces are expected to emerge. Geo-radar measures should be carried out in the boreholes as needed.

9 CONCLUSION

This GG elaborate provides vital results from the extensive multi-year geological, geotechnical, hydrogeological, and geophysical investigations in the T1 and T2 tunnels that the designer will need to prepare the project documentation. The elaborate represents a synthesis of several reports cited in references [2] to [8]. Those also provide all the data and results based on which interpretations were made.

Despite extensive investigations, due to the complexity of the investigated area, which is conditioned by the structural tectonic history of the area, and the fact that the route mostly passes through karst terrain and below groundwater levels, no definitive answer can be given to all questions. Therefore, geologically geotechnical conditions are always estimated, but in some places, there may be some changes, especially in terms of predicted contacts between individual units - they may occur slightly sooner or later than the announced chainages. In particular, deviations are possible within the karst prediction due to its selective and virtually unpredictable nature of occurrence in a broader area.

The designer will have to take into account the possibility of different BT and GT units appearing on individual sections, as shown on the longitudinal GG profiles in Annex G.2. In this way, all possible scenarios and support measures will be addressed during the excavation phase. Appropriate geological and geotechnical monitoring during the construction phase will further reduce the risks.

10 REFERENCES

[1] Končni elaborat o izvedbi strukturno geoloških, hidrogeoloških, krasoslovnih in geotehniških raziskav; faza PZI, GeoZS & IRGO Consulting & GIZRMK & ZRC SAZU, September 2018.

[2] Geološko-geotehnični elaborat s sintezo vseh preiskav za predor T1 (PGD dop.), 2019, ELEA, ZAG

[3] Geološko-geotehnični elaborat s sintezo vseh preiskav za predor T2(PGD dop.),2019, IRGO Consulting, ELEA

[4] GG elaborat za predor T1; faza PGD, IRGO Consulting, Elea IC, November 2010

[5] GG elaborat za predor T2; faza PGD, IRGO Consulting, Elea IC, November 2010

[6] GG elaborat za predor T2-dodatna vrtina (T2-13a) ; faza PGD, IRGO Consulting, Elea IC, November 2010

[7] GG elaborat – objekti preko doline Glinščice, faza PGD, ZRMK, 2011

[8] GG elaborat – geotehnični objekti preko doline Glinščice (most Glinščica 1, most Glinščica 2, in galerija Glinščica), faza PZI, IRGO Consulting, Februar 2018

[9] Hoek E.: A discussion on acceptable criteria for temporary support and final linings of large span transportation tunnels in poor rock, - Vancouver, March 1999.

Annex 1

Basic information about the boreholes performed

Table 12: Basic design (PGD) phase

borehole ident	obejct	chainage		depth (m)	monitoring	X	Y	Z	investigations	PERFORMANCE		
										enterprise in charge (date of performance)	number of presiometres	number of slug tests
T1-1	Tunnel T1	km	3+006	35	ZAG	58007,13	418107,94	424,78	pressiometer: 7- 10 m whole section overviewed by camera	GEOT (26.5.-3.6.2010)	1	
T1-2	Tunnel T1	km	3+006	35	ZAG	58009,06	418100,55	425,42	pressiometer: 10-13 m whole section overviewed by camera whole core preserved	GEOT (11.3.- 24.3.2010)	1	
T1-3	Tunnel T1	km	3+006	36	ZAG	58025,00	418081,72	428,03	whole core preserved	GEOT (28.4.- 25.5.2010)	2	
T1-4	Tunnel T1	km	3+082	35	ZAG	57948,43	418064,08	421,62	pressiometer: 4-7 m	GEOT (16.3.- 26.3.2010)	1	
T1-5	Tunnel T1	km	3+082	35	ZAG	57951,48	418055,85	421,54	pressiometer: 6-8 m; inclinometre	GEOT (26.3.-8.4.2010)	1	
T1-6	Tunnel T1	km	3+082	35	ZAG	57958,15	418045,32	421,82	pressiometer: 6-9,10-13,27-30 m whole section overviewed by camera well logging	GEOT (9.4.-26.4.2010)	3	
T1-7	Tunnel T1	km	4+890	350	ZAG	56369,81	417186,3	586,62	pressiometer: 190-200 piezometer whole core preserved	-	3	
T1-8	Tunnel T1	km	6+740	275	ZAG	54757,8	416277,91	596,28	pressiometer: 235-245 m; well logging, piezometer; whole core preserved	CROSCO (8.6.- 5.7.2010)	3	
T1-9	Tunnel T1	km	8+265	160	ZAG	53500,15	415418,38	457,82	pressiometer: 122-132 m; well logging; georadar measurements	CROSCO (9.7.- 25.7.2010)	3	
T1-10	Tunnel T1	km	8+745	150	ZAG	53121,14	415117,83	443,14	pressiometer: 80-83, 112-115, 147-150 m; well logging, piezometer; whole core preserved	CROSCO (22.4.- 10.5.2010)	3	
T1-11	Tunnel T1	km	9+400	100	ELEA	52577,81	414730,35	375,85	pressiometer: 72-75, 82-85, 92- 95 m; whole core preserved	CROSCO (6.05.2010)	3	
T1-12	Tunnel T1	km	9+635	25	ELEA	52377,67	414633,82	308,7	seizmic dilatometer	IMPREFOND (16.06. - 21.06.2010)		

borehole ident	obejct	chainage		depth (m)	monitoring	X	Y	Z	investigations	PERFORMANCE		
										enterprise in charge (date of performance)	number of presiometres	number of slug tests
T1-13	Tunnel T1	km	9+630	30	ELEA	52399,08	414609,1	318,69	inclinometer pressiometer: 5-8, 10-13, 15- 18m; whole core preserved	ROVS (21.06. - 29.06.2010)	3	
T1-14	Tunnel T1	km	9+660	20	ELEA	52365,66	414591,33	304,65	-	IMPREFOND (09.06. - 15.06.2010)		
T1-15	Tunnel T1	km	9+660	30	ELEA	52390,51	414555,51	313,55	pressiometer: 5-8, 10-13, 15- 18m inclinometer; whole core preserved	ROVS (14.06. - 21.06.2010)	3	
T1-16	Tunnel T1	km	9+665	30	ELEA	52376,14	414573,85	309,74	-	ROVS (07.6. - 11.06.2010)		
T1-17	Tunnel T1	km	9+690	20	ELEA	52379,05	414539,98	306,98	-	ROVS (31.5. - 04.06.2010)		
T2-16	Tunnel T2	km	9+906	20	ELEA	52212,68	414419,93	301,31	-	ROVS (21.07.2010) - 28.07.2010)		
T2-17	Tunnel T2	km	9+942	35	ELEA	52150,16	414399,29	318,41	inclinometer	ROVS (29.07.2010) - 06.08.2010)		
T2-18	Tunnel T2	km	9+950	30	ELEA	52139,79	414412,56	306,57	pressiometer: 5-8, 10-13, 15-18m	ROVS (09.08.2010)	3	
T2-19	Tunnel T2	km	9+948	25	ELEA	52109,12	414457,2	305,83	inclinometer	ROVS (08.07.2010) - 13.07.2010)		
T2-20	Tunnel T2	km	9+970	15	ELEA	52112,83	414431,75	294,89	seizmic dilatometer	ROVS (06.07.2010) - 07.07.2010)		
T2-21	Tunnel T2	km	9+980	30	ELEA	52084,86	414439,86	309,98	pressiometer: 5-8, 10-13, 15-18m	ROVS (14.07.2010) - 20.07.2010)	3	
T2-7	Tunnel T2	km	10+600	160	ELEA	51563,3	414160,86	405,49	VDP-slug test na 130-135, 140-145m well logging video shooting pressiometer: 120-123, 130-133, 140-143m	IMPREFOND (05.07.2010) - 05.08.2010)	3	2

borehole ident	obejct	chainage		depth (m)	monitoring	X	Y	Z	investigations	PERFORMANCE		
										enterprise in charge (date of performance)	number of presiometres	number of slug tests
T2-8	Tunnel T2	km	11+225	150	ELEA	50940,37	414028,97	393,81	VDP-slug test na 95-100, 115-120m well logging video shooting pressiometer: 100-103, 110-113, 120-123m	IMPREFOND (14.06.2010) - 16.07.2010)	3	2
T2-9	Tunnel T2	km	11+830	170	ELEA	50392,91	413862,99	396,65	piezometer georadar video shooting well logging pressiometer: 130-133, 150-153, 167-170m	IMPREFOND (09.06.2010) - 02.07.2010)		
T2-10	Tunnel T2	km	12+530	200	ELEA	49665,07	413653,52	431,22	piezometer video shooting well logging pressiometer: 170-173, 180-183, 190-193m	IMPREFOND (20.07.2010) - 25.10.2010)		
T2-11	Tunnel T2	km	13+300	250	ELEA	48947,33	413440,44	428,39	VDP-nalivalni test na 195-200, 215-220m piezometer georadar well logging video shooting pressiometer: 170-173, 190-193, 210-213m	IMPREFOND (28.05.2010) - 25.06.2010)	1	2
T2-12	Tunnel T2	km	13+591	226	IRGO	48660,1	413360,85	426,9	piezometer well logging video shooting pressiometer 189-193m	CROSCO (22.05.2010) - 18.06.2010)	1	

borehole ident	obejct	chainage		depth (m)	monitoring	X	Y	Z	investigations	PERFORMANCE		
										enterprise in charge (date of performance)	number of presiometres	number of slug tests
T2-13	Tunnel T2	km	14+240	251	IRGO	48040,42	413183,59	411,92	Slug test: 184,8-190, 200-205,5m piezometer well logging video shooting pressiometer: 180-185, 196-199, 201-204m	CROSCO (19.06.2010) - 08.07.2010)	3	2
T2-14	Tunnel T2	km	14+583	227	IRGO	47707,8	413088,56	401,85	well logging video shooting pressiometer: 166-168, 185-188, 190-192m	CROSCO (11.05.2010) - 07.06.2010)	3	
T2-15	Tunnel T2	km	15+733	130	IRGO	46652,48	412637,27	286,48	Slug test: 55-67, 81-90m piezometer well logging video shooting pressiometer: 41-43, 50-52, 59-61, 68-69, 75-77m	CROSCO (11.05.2010) - 07.06.2010)	4	2
T1a-1	Gallery Glinščica	km	9+770	20	ZRMK	52286,7	414520,85	295,57	pressiometer: 6-9, 13-16m	(24.8.2010)	2	
T1a-2	Gallery Glinščica	km	9+790	20	ZRMK	52270,88	414507,76	298,84	inclinometer, pressiometer: 4-9, 9-12m	(21.9.2010)	2	
T1a-3	Gallery Glinščica	km	9+800	20	ZRMK	52254,46	414511,38	302,34	inclinometer	(21.6.2010)		
T1a-4	Gallery Glinščica	km	9+800	15	ZRMK	52258,12	414502,94	295,68	-	(1.9.2010)		
GL/V2-1	Gallery Glinščica	km	9+690	20	ZRMK	52366,08	414554,8	303,67	pressiometer: 5-8, 10-13, 15-18m	(24.6.2010)	3	

borehole ident	obejct	chainage		depth (m)	monitoring	X	Y	Z	investigations	PERFORMANCE		
										enterprise in charge (date of performance)	number of presiometres	number of slug tests
GL/V2-2	Gallery Glinščica	km	9+710	15	ZRMK	52353,94	414520,59	228,89	pressiometer: 3-6, 10-13, 15-18m	(29.6.2010)	3	
GL/V2-3	Gallery Glinščica	km	9+760	15	ZRMK	52298,9	414524,86	288,52	-	(14.9.2010)		
GL/V2-4	Gallery Glinščica	km	9+765	20	ZRMK	52295,18	414513,31	288,44	pressiometer: 3-6, 10-13, 15-18 m	(1.9.2010)	3	
GL/V3-1	Gallery Glinščica	km	9+820	20	ZRMK	52244,96	414486,38	283,82	pressiometer: 3-6, 9-12, 15-18	(6.8.2010)	3	
GL/V3-2	Gallery Glinščica	km	9+840	20	ZRMK	52221,76	414477,19	283,47	-	(18.8.2010)		
GL/V3-3	Gallery Glinščica	km	9+880	15	ZRMK	52185,65	414452,17	278,92	pressiometer: 3-6, 11-14	(23.7.2010)	2	
GL/V3-4	Gallery Glinščica	km	9+885	20	ZRMK	52175,73	414448,34	280,02	-	(16.7.2010)		

Table 13: Basic design (PGD_{dop}) phase

borehole ident	obejct	chainage		depth (m)	monitoring	X	Y	Z	investigations	PERFORMANCE		
										enterprise in charge (date of performance)	number of presiometres	number of slug tests
T1-12/17	Tunnel T1	km	4+650	250	ZAG	56582,31	417298,46	591,34	well logging measurements, camera shooting, georadar	GroundEngineering d.o.o. (21.03. - 13.04.2018)		3
T1-13/17	Tunnel T1	km	6+287	350	ZAG	55147,70	416506,81	597,48	karotažne meritve, snemanje s kamero	Geotec S.p.A. (31.03. - 16.05.2018)		2
T1-14/17	Tunnel T1	km	7+500	260	ZAG	54133,50	415840,48	525,68	well logging measurements, camera shooting, georadar	GroundEngineering d.o.o. (05.01. - 28.01.2018)		2
T1-15/17	Tunnel T1	km	8+900	200	ZAG	52949,52	415059,04	411,56	well logging measurements, camera shooting, georadar	Geotec S.p.A. (17.11. - 11.12.2018)		3
T2-16/17	Tunnel T2	km	10+800	250	ELEA	51336,11	414139,47	428,72	well logging measurements	Geotec S.p.A. (18.12.2017-22.1.2018)		3
T2-17/17	Tunnel T2	km	11+281	150	ELEA	50871,72	414022,04	377,14	well logging measurements, camera shooting, georadar	Geotec S.p.A. (24.1.-.12.2.2018)		3
T2-18/17	Tunnel T2	km	12+045	200	IRGO	50095,76	413818,09	407,63	well logging measurements, camera shooting, georadar	Geotec S.p.A. (22.2.-14.3.2018)		2
T2-19/19	Tunnel T2	km	5+350	300	IRGO	47023,56	412870,13	354,89	well logging measurements, camera shooting, georadar	GroundEngineering d.o.o. (18.2.-16.3.2018)		3
T2-20/17	Tunnel T2	km	5+650	150	IRGO	46758,3	412720,58	150,00	well logging measurements, camera shooting, georadar	GroundEngineering d.o.o. (31.1.-14.2.2018)		3
T-2a/V-1	Access road T-2a	km	out of tunnel axis	10	ELEA	51987,37	414525,91	359,26	pressiometer: 4-7, 7-0m	Geotrans (10.10.2017)	2	
T-2a/V-2	Access road T-2a	km	out of tunnel axis	10	ELEA	51966,25	414452,32	347,44	-	Geotrans (11.10.2017)		
T-2a/V-5	Access road T-2a	km	out of tunnel axis	17	ELEA	52134,58	414497,1	299,82	pressiometer: 3-6, 6-8, 10-13m	Geotrans (8.11.2017)	3	
T-2a/V-6	Access road T-2a	km	out of tunnel axis	17	ELEA	52115,36	414487,18	294,95	pressiometer: 5-7, 10-13	Geotrans (24.10.2017)	2	

borehole ident	obejct	chainage		depth (m)	monitoring	X	Y	Z	investigations	PERFORMANCE		
										enterprise in charge (date of performance)	number of presiometres	number of slug tests
GL/V-1	Gallery Glinščica	km	9+690	22	IRGO	52361,12	414555,43	298,92	pressiometer: 5-7, 19-22m	Geotrans (9.1.2018	2	
GL/V-2	Gallery Glinščica	km	9+785	12	IRGO	52269,11	414520,73	304,26	pressiometer: 4-7, 7-10, 10-12m	Geotrans (21.11.2017)	3	
GL/V-3	Gallery Glinščica	km	9+780	18	IRGO	52278,1	414502,53	293,87	pressiometer: 5-7, 15-18m	Geotrans (28.11.2017)	2	
GL/V-4	Gallery Glinščica	km	9+805	15	IRGO	52261,57	414493,23	288	pressiometer: 4-7, 12-15m	Geotrans (17.11.2017)	2	
GL/V-5	Gallery Glinščica	km	9+905	13	IRGO	52170,72	414446,84	280,48	pressiometer: 4-7, 10-13m	Geotrans (10.11.2017)	2	

Annex 2

An overview of analysis of selected parameters

As part of the analysis and selection of geomechanical parameters, more than 5,000 borehole log, field, and lab survey data have been reviewed and statistically processed. The results of the statistical processing are, for ease of understanding, presented in the form of spreadsheets, bar charts, and in the form of, e.g., Boxplot or box diagrams. The number of samples analysed is shown in the diagram (n=*). Data where the number of samples is less than 5 (n <5) are not considered statistically representative but are nonetheless informative.

Protocols for conducting field and lab investigations and their interpretation are given in the reports of the annexes. There are presented field investigations carried out in the form of studies of tunnels T1 and T2 and other references [1] to [6]. Studies for the Glinščica area are presented in references [7] and [8].

1. Volume weight

Soils

A total of fourteen soil samples and heavily weathered GT0 type rocks were analyzed in the lab, of which five samples of unit 0a and nine samples of unit 0b and four samples of karst cavern filling, marked K, which were not taken into account in further processing.

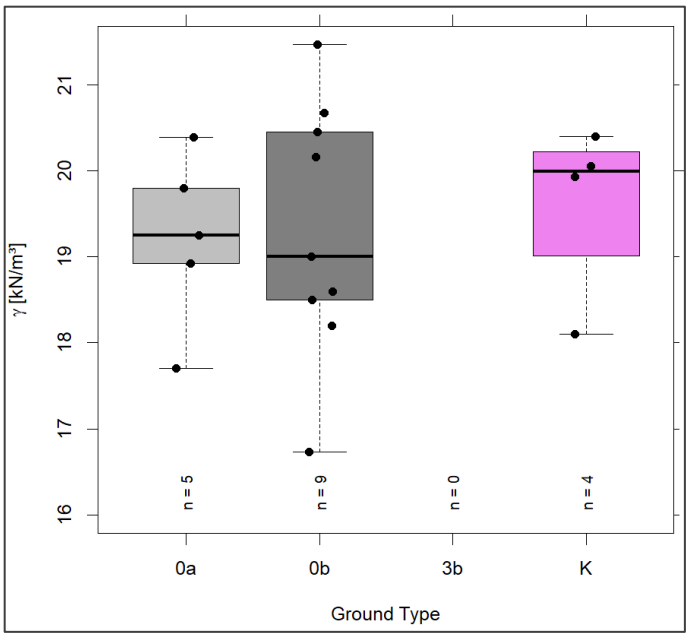

	n	Min.	1st Qu.	Median	Mean	3rd Qu.	Max.	Sd
0a	5	17,70	18,92	19,25	19,21	19,80	20,39	1,01
0b	9	16,73	18,50	19,00	19,31	20,45	21,47	1,49
K	4	18,10	19,02	19,99	19,62	20,23	20,40	1,03
total	18	16,73	18,50	19,53	19,35	20,39	21,47	1,22

Figure 14: Results of soil volume analysis by rock mass types

The selected value of 19 kN/m^3 of unit 0a corresponds to both the median and the mean value and is reasonable given the knowledge of these and similar materials. The results of the value of unit 0b are probably too low since these are heavily weathered rock mass, where the structure is still partially preserved. It is mainly attributed to the fact that the worst pieces were taken for the lab analysis, which does not show the observed conditions when inspecting the cores of the boreholes and field status. According to the acquaintance with the present material, it was decided to maintain the volume weight of 23 kN/m^3, which was determined in the previous stages of research and analysis.

Rock

Two hundred fifty-four volume tests of rock samples were carried out. A statistical overview of data distribution was made by aggregation as by lithological units as by rock mass types.

The results show that the volume weight values for all lithological units are ranging ca. 26 kN/m^3. That is consistent with the analysis of the volume weight by GT units and the statistical processing of data in the PGD_{dop} phase (Figures 15, 16, and 17).

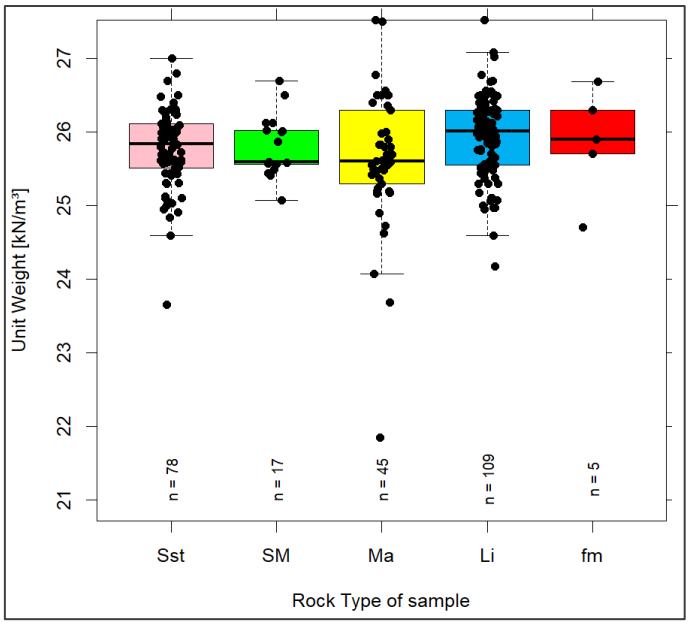

	n	Min.	1st Qu.	Median	Mean	3rd Qu.	Max.	sd
Sst	78	23,7	25,5	25,8	25,8	26,1	27,0	0,5
SM	17	25,1	25,6	25,6	25,8	26,0	26,7	0,4
Ma	45	21,9	25,3	25,6	25,6	26,3	27,5	0,9
Li	109	24,2	25,6	26,0	25,9	26,3	27,5	0,5
fm	5	24,7	25,7	25,9	25,9	26,3	26,7	0,7
total	254	21,9	25,5	25,9	25,8	26,3	27,5	0,6

Figure 15: Results of volume analysis by lithological units

Lithology		Density (kg/m3)
marlstone	n	13
	min	2519
	max	2650
	average	2606
	standev	35
	charact.value 95%	**2581**
sandstone	n	51
	min	2510
	max	2698
	average	2639
	standev	37
	charact.value 95%	**2627**
alternating layers of marlstone, siltstone and sandstone	n	13
	min	2575
	max	2664
	average	2625
	standev	27
	charact.value 95%	**2606**
marlstone, siltstone/ transitional layers	n	41
	min	2438
	max	2712
	average	2596
	standev	51
	charact.value 95%	**2578**
limestone	n	129
	min	2370
	max	2754
	average	2654
	standev	51
	charact.value 95%	**2644**

Figure 16: Results of rock mass volume weight from PDG_{dop} phase

γ					
mean	max	min	st.dev.	GT	no.
25,72	26,80	23,66	0,59	1a	36,00
25,86	26,40	25,04	0,36	1b	23,00
25,71	26,70	24,91	0,44	2a	17,00
25,92	27,00	24,60	0,57	2b	18,00
26,04	27,53	25,17	0,77	3a	16,00
25,31	26,50	21,85	1,04	3b	23,00
25,93	27,09	24,18	0,54	4a	68,00
25,99	27,53	24,97	0,52	4b	44,00
26,10	26,30	25,90	0,28	5a	2,00
25,62	26,69	24,71	0,83	5b	4,00

Figure 17: Results of volume analysis by rock mass type

2. Uniaxial compressive strength

Soils

In the lab, a total of eight samples of uniaxial compressive strength of soil were examined, of which two were samples of unit 0a, four samples of unit 0b, and two samples of karst fillings (K). Due to the insufficient number of samples, they are not considered statistically representative and have not been added to the selected parameter table.

Rock

The data show that 189 examinations of uniaxial pressure samples of rock were carried out in the lab. The statistical distribution of the data was obtained by grouping by lithological units.

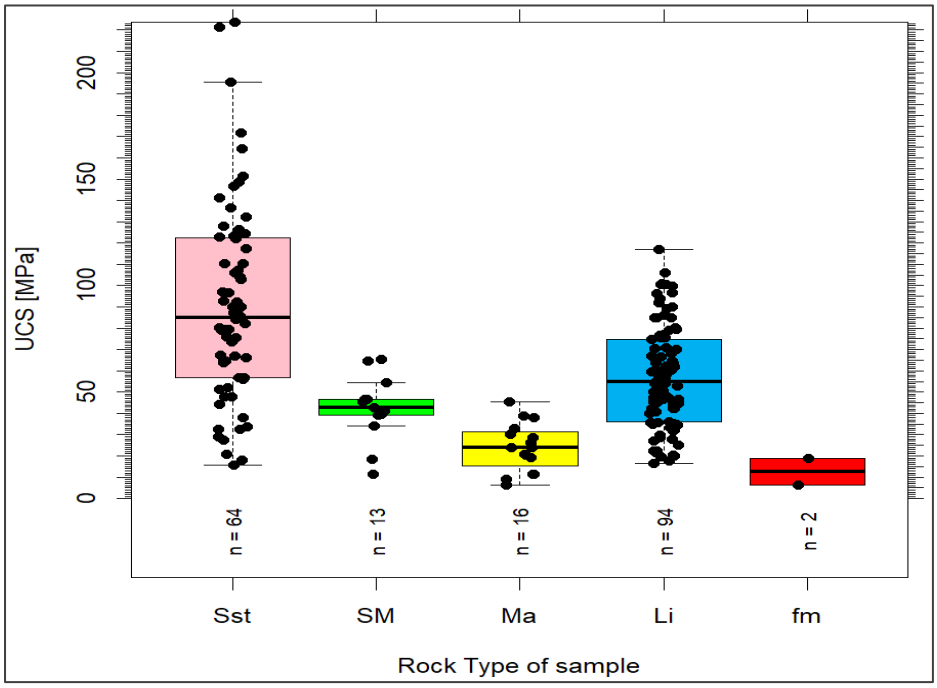

	n	Min.	1st Qu.	Median	Mean	3rd Qu.	Max.	sd
Sst	64	15,9	56,7	84,9	91,1	122,4	223,9	46,7
SM	13	11,5	39,2	42,5	42,3	46,8	65,2	15,4
Ma	16	6,3	15,4	24,0	24,2	31,6	45,4	11,3
Li	94	16,4	35,9	54,6	56,7	74,6	117,1	23,8
fm	2	6,3	6,3	12,5	12,5	18,8	18,8	8,9
total	189	6,3	35,5	56,7	64,1	84,7	223,9	38,9

Figure 18: Results of the analysis of an uniaxial compressive strength results vs. lithology

When choosing lab parameters, the assumption was made that tectonically less damaged rock mass has a higher strength. Therefore the values of 1st quartile (units a) are selected, while the strengths of tectonically medium and high damaged rocks are lower due to cracking and deterioration of the entire structure of the rocks, so the 3rd quartile values are selected. The values indicate the range within which the strengths of the individual units appear.

For units 5a and 5b, only two strength tests were performed, so they are not considered statistically representative, and the minimum value of the bedrock was assumed as the characteristic value; in case of 5a -

limestone, as lower than the value of sandstone and limestone, and in case of 5b - marlstone. For further calculations, lower values of the statistical processing of the PGD_{dop} phase were selected in the table of parameters selected.

The proposed characteristic uniaxial compressive strength of the intact rocks is summarized based on of the analysis of the lab investigations of the PGD_{dop} phase. Except for units 5a and 5b, where the values of the bedrock 5a - sandstone are taken as characteristic values, as being lower than the values of sandstone and limestone, and in the case of 5b - marlstone (Figures 18 and 19).

Lithology		Uniaxial compressive strength	Equivalent of uniaxial compressive strength
		(MPa)	(MPa)
marlstone	n	13	-
	min	5,08	-
	max	32,90	-
	average	20,83	-
	standev	7,84	-
	charact.value 95%	**15,26**	-
sandstone	n	44	14
	min	20,83	14,80
	max	221,26	92,70
	average	76,36	53,30
	standev	41,54	21,46
	charact.value 95%	**61,82**	**38,77**
alternating layers of marlstone, siltstone and sandstone	n	12	-
	min	20,83	-
	max	85,54	-
	average	50,50	-
	standev	19,62	-
	charact.value 95%	**35,82**	-
marlstone, siltstone/ transitional layers	n	28	-
	min	5,79	-
	max	62,50	-
	average	27,42	-
	standev	16,97	-
	charact.value 95%	**19,81**	-
limestone	n	131	20
	min	9,15	19,30
	max	158,08	108,40
	average	70,41	58,73
	standev	30,44	27,58
	charact.value 95%	**64,38**	**43,72**

Figure 19: Results of volume analysis of rock mass from the PGD_{dop} phase

3. Parametre RQD

RQD values were determined based on of borehole inventory, and for most boreholes the value of RQD was already determined at the stage of implementation of borehole inventory in the field. In particular, in the boreholes of older stages, it was found that the RQD values were determined incorrectly or incorrectly as a result of disregarding core damage due to drilling. Where possible, such valuations were revised, but where, in our estimation, real revaluation could not be made either due to missing images or due to unfamiliarity with the work being done; they were not taken into account in further analysis. Statistical evaluation was performed for rock mass types based on more than 4,600 data (Figure 20).

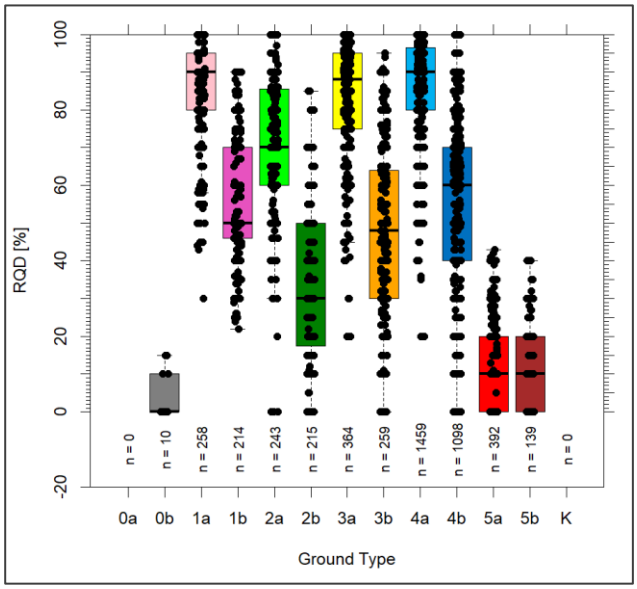

	n	Min.	1st Qu.	Median	Mean	3rd Qu.	Max.	sd
1a	258	30,0	80,0	90,0	85,0	95,0	100,0	14,3
1b	214	22,0	46,0	50,0	57,1	70,0	90,0	17,6
2a	243	0,0	60,0	70,0	70,8	85,5	100,0	20,6
2b	215	0,0	17,5	30,0	32,4	50,0	85,0	21,1
3a	364	20,0	75,0	88,0	83,5	95,0	100,0	15,6
3b	259	0,0	30,0	48,0	47,7	64,0	95,0	22,8
4a	1459	20,0	80,0	90,0	87,9	96,5	100,0	11,4
4b	1098	0,0	40,0	60,0	55,5	70,0	100,0	21,0
5a	392	0,0	0,0	10,0	13,7	20,0	43,0	12,3
5b	139	0,0	0,0	10,0	11,8	20,0	40,0	11,7
total	4651	0,0	40,0	70,0	63,9	90,0	100,0	29,9

Figure 20: Results of the statistical analysis of RQD distribution

4. Parametre GSI, m_i and D

The GSI (Geological Strength Index) parameters were evaluated based on the inventory and photographs of boreholes where possible. The analysis of the distribution of GSI parameters was performed by rock mass types and the results are shown in Figure 21.

mean	max	min	st.dev.	GT	no.	95%
79,47	95,00	45,00	12,22	1a	212,00	79,47
55,60	79,50	25,00	11,13	1b	154,00	55,60
68,63	95,00	21,00	13,13	2a	207,00	68,63
40,72	65,00	5,00	10,83	2b	181,00	40,72
76,46	95,00	42,50	10,79	3a	363,00	76,46
46,69	77,50	18,00	10,91	3b	254,00	46,69
83,02	95,00	40,00	7,88	4a	1434,00	83,02
56,91	90,00	15,00	11,35	4b	1091,00	56,91
25,61	47,00	5,00	7,93	5a	381,00	25,61
15,92	37,00	0,00	8,64	5b	127,00	15,92

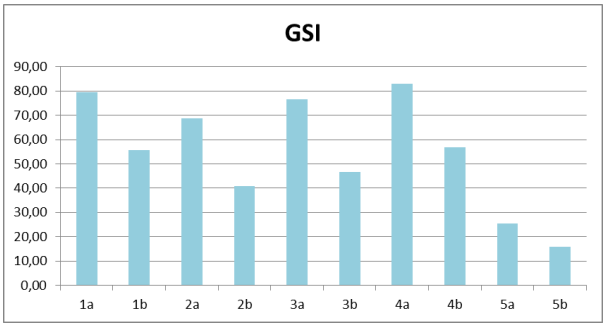

Figure 21: Results of the statistical analysis of GSI distribution

The values of the material constant m_i and the blast damage factor D were determined according to the literature proposal for the use of RocLab by Rocscience, with the default blast damage factor D = 0.2 in the first 0.5 to 1.0 m of rock mass in areas where it excavation by blasting is expected and D = 0.0 in areas where mechanical excavation is expected.

5. Shear charachteristics

Soil

The shear characteristics of the soil unit 0a were analyzed based on the results of lab direct shear tests. The shear values of unit 0b were determined on the base of a comparison of the lab tests results and by means of feedback stability analyzes for the portal area (Figure 22).

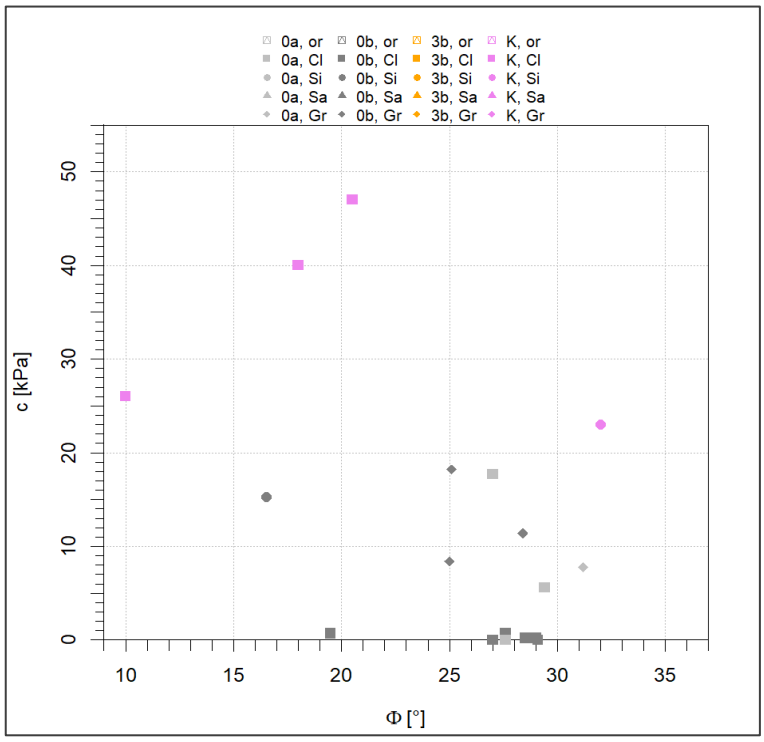

φ [°]	n	Min.	1st Qu.	Median	Mean	3rd Qu.	Max.	Sd
Cl	13	10,00	20,50	27,00	24,63	28,50	29,40	5,86
Si	2	16,50	16,50	24,25	24,25	32,00	32,00	10,96
Gr	4	25,00	25,05	26,75	27,43	29,80	31,20	2,97
total	19	10,00	22,75	27,00	25,18	28,75	32,00	5,70

c [kPa]	n	Min.	1st Qu.	Median	Mean	3rd Qu.	Max.	Sd
Cl	13	0,00	0,00	0,70	10,62	17,70	47,00	16,74
Si	2	15,30	15,30	19,15	19,15	23,00	23,00	5,44
Gr	4	7,80	8,10	9,90	11,45	14,80	18,20	4,77
total	19	0,00	0,20	7,80	11,69	17,95	47,00	14,12

Figure 22: Results of the statistical analysis of the shear characteristics of the soil

Rock

The shear characteristics of the rock masses are calculated based on the Hoek-Brown criterion. The required parameters are given in the table with characteristics.

6. Elastic parameters

The elastic parameters of the rock mass were analysed based on lab tests and field measures. The results of analyses are given further on.

6.1.1. Lab

Based on the analysis of 75 samples of lab tests of elastic rock properties by typical lithological units, the values of tectonically intact and slightly damaged rock values for the 3rd quartile and for the tectonic medium to severely damaged quartile values of the 1st quartile are given (Figure 23).

As default value of the intact rock for further calculations, a value of tectonically low to the non-failure rock mass (3rd quartile) should be accepted, except in the case of the GT2 unit, where the influence of the sandstone layer increases the strength and the default value of the intact rock was the median value.

Only two samples were analysed for units 5a and 5b, so they are not considered statistically representative, and the results are not added to the parameter table. In the case of the recommended value of the intact rock elastic modulus, the default values are taken in the 5a case – of sandstone as lower than the values of sandstone and limestone, and in the 5b case – of marlstone. The results are also comparable to the results of the PGD_{dop} phase analysis, which is considered as confirmation of the selected parameters.

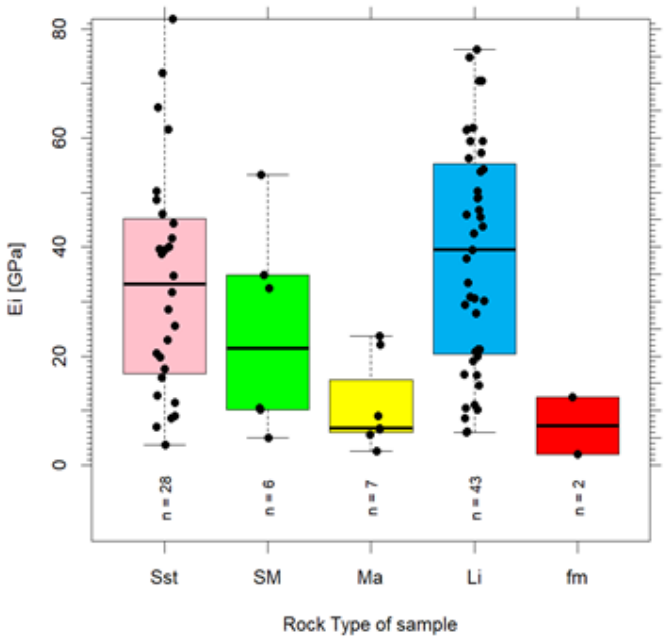

	n	Min.	1st Qu.	Median	Mean	3rd Qu.	Max.	sd
Sst	24	3692,0	14377,0	27010,0	27436,5	39823,0	50229,0	14671,8
SM	6	4964,0	10150,0	21387,5	24329,2	34800,0	53286,0	18883,6
Ma	7	2500,0	6016,5	6667,0	10865,6	15579,5	23700,0	8459,4
Li	36	5955,0	17833,5	30700,0	32643,6	47871,5	59465,0	17148,3
fm	2	1950,0	1950,0	7175,0	7175,0	12400,0	12400,0	7389,3
total	75	1950,0	11263,0	25520,0	27600,4	42006,0	59465,0	16960,0

Lithology		Young's modulus (MPa)
marlstone	n	8
	min	6533
	max	23700
	average	13506
	standev	7415
	charact.value 95%	**6058**
sandstone	n	16
	min	17636
	max	81917
	average	35780
	standev	15543
	charact.value 95%	**26105**
alternating layers of marlstone, siltstone and sandstone	n	2
	min	10150
	max	19788
	average	14969
	standev	6815
	charact.value 95%	-
marlstone, siltstone/ transitional layers	n	15
	min	2500
	max	41175
	average	25594
	standev	10284
	charact.value 95%	**18930**
limestone	n	48
	min	5955
	max	109349
	average	58155
	standev	28739
	charact.value 95%	**48549**

Figure 23: Results of the statistical analysis of lab results of elastic modules and analysis of parameters from the PGD_{dop} phase

6.1.2. Elastic properties of rock mass (E_{rm})

Using the RocLab program of the Rocscience enterprise, we have calculated the elastic properties of the rock mass by the Hoek-Brown criterion theory. In the calculations, the values used were given in the previous columns of the spreadsheet with the parameters:

- Intact uniaxial strength (sci),
- GSI index (min in max),
- Constants mi and blast damage factor D,
- Elastic Intact Rock Module (Ei).

The calculations were made using the applicable minimum and maximum GSI values to obtain the predicted range of elastic modulus of rock mass by rock mass types.

6.1.3. Field investigations

The analysis of the field investigation results of the elastic modules covered the processing of the pressiometer measure results. Measures were taken in both deep boreholes and shallow boreholes on portals. The distribution of investigations with values of load modulus is shown in the tables below (referred to as Table 24).

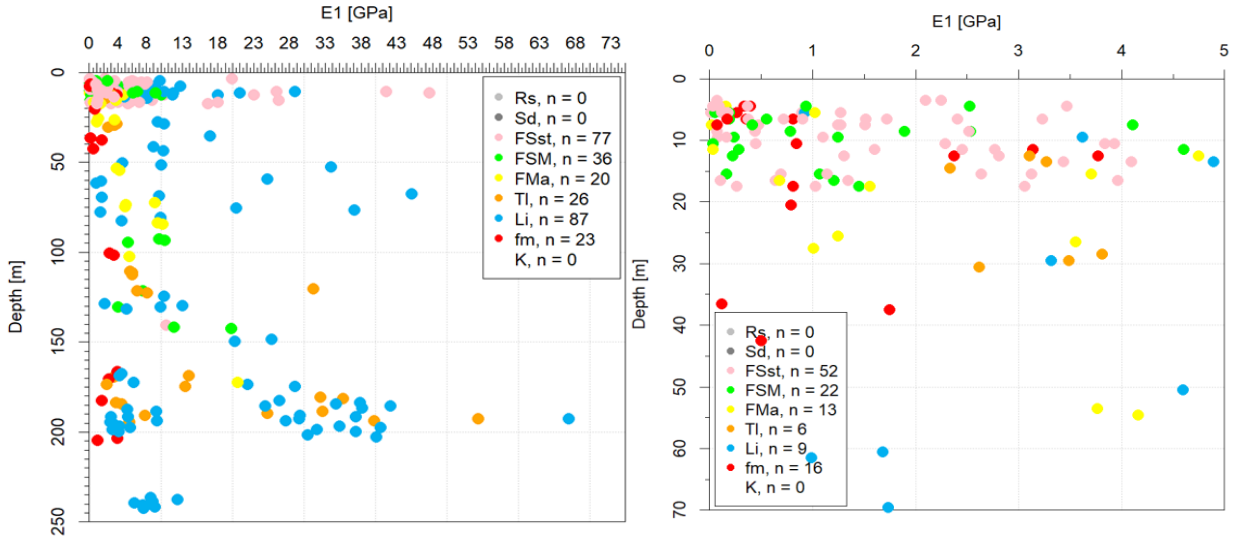

Figure 24: Distribution of loaded elastic modulus values by depth

Despite a large amount of data, it has been shown that for some rock mass types, the data is much more prevalent, while for others, it is less. The deficiency mainly turns out in some flysch units (e.g., 1b), where the representation by boreholes where measures were taken is smaller and in units 5a and 5b where measure is difficult to ensure adequate stability in disturbed materials.

The tables below show the measurements used for determining the parameters:

GT: 1a			
borehole	**depth**	**E1**	**E2**
T2-18	10,6	41535,9	38882,3
T2-18	11,5	47572,4	70300,8
T2-18	12,4	10467,0	29528,5
T2-18	15,7	26500,6	35786,3
T2-18	17,6	16525,2	24626,3
T2-8	120,9	31344,5	54591,7
n		5,0	5,0
min		10467,0	24626,3
max		47572,4	70300,8
average		28520,2	39824,8
stand.deviation		15860,9	17909,4
charact. value 90% (Fellin, 2005)		**20127,7**	**28105,7**

GT: 1b			
borehole	**depth**	**E1**	**E2**
T2-18	16,7	5702,0	11634,6

GT:2a			
borehole	depth	E1	E2
T1-11	92,0	9766,5	13895,8
T1-11	93,0	10545,8	12666,2
T2-21	10,8	9426,5	17069,8
T2-7	121,0	10797,3	18006,9
T2-7	140,8	10695,1	25500,7
T2-7	141,5	11796,9	28668,7
T2-7	142,3	19791,8	22960,5
T2-21	10,0	9426,5	17069,8
T2-21	12,0	9993,6	21568,5
n		9,0	9,0
min		9426,5	12666,2
max		19791,8	28668,7
average		11360,0	19711,9
stand.deviation		3251,8	5339,4
charact. value 90% (Fellin, 2005)		8377,6	14814,7

GT: 2b			
borehole	depth	E1	E2
T2-21	11,0	4597,9	11914,7
T2-07	130,0	3960,5	5538,3
T1-11	94,0	5375,7	9894,7
T2-7	121,7	6924,4	20971,9
T2-7	122,4	4703,7	9981,9
T2-7	130,4	6535,8	8898,7
n		6,0	6,0
min		3960,5	5538,3
max		6924,4	20971,9
average		5349,6	11200,0
stand.deviation		1166,1	5225,7
charact. value 90% (Fellin, 2005)		3843,6	4451,3

GT: 3a			
borehole	depth	E1	E2
T2-21	10,8		
T2-21	11,5	4597,9	11914,7
T2-21	12,3	9993,6	21568,5
T2-21	15,9	1068,3	1918,3
T2-21	16,6	1202,5	1791,9
T2-21	17,3	1450,9	2048,4
T2-8	100,7	2855,3	5518,7
T2-8	101,4	3384,3	5291,7
T2-8	102,1	5598,7	6774,8
T2-8	110,8	5688,8	10702,7
T2-8	111,6	5945,1	6245,2
T2-8	112,4	6020,4	9255,9
T2-8	121,6	6647,6	8372,1
T2-8	122,3	8034,0	11761,1
T1-11	72,0	9107,2	11266,4
T1-11	73,0	5144,6	10027
T1-11	74,0	5004,6	12700,4
T1-11	83,0	9503,2	18930,2
T1-11	84,0	10240	13895,8
n		18,0	18,0
min		1068,3	1791,9
max		10240,0	21568,5
average		5638,2	9443,5
stand.deviation		2938,3	5451,4
charact. value 90% (Fellin, 2005)		3935,8	6285,1

GT: 3b			
borehole	depth	E1	E2
T2-2	12,0	3106,0	6341,3
T2-2	13,0	3267,3	
T2-2	14,0	2333,7	9790,2
T2-3	15,0	3702,7	12867,6
T2-3	16,0	672,9	2639,1
T2-2	28,0	3811,1	
T2-2	29,0	3486,2	
T2-2	30,0	2614,1	5616,0
T2-1	53,0	3760,8	10574,3
T2-1	54,0	4157,4	14044,7
n		10,0	7,0
min		672,9	2639,1
max		4157,4	14044,7
average		3091,2	8839,0
stand.deviation		1017,3	4129,3
charact. value 90% (Fellin, 2005)		2448,0	6640,7

GT: 4a			
borehole	depth	E1	E2
T2-15	59,9	27924,9	36127,8
T2-15	67,0	45065,4	52589,6
T2-15	75,8	20561,5	24457,9
T2-15	76,5	37056,6	42823,5
T1-3	10,0	28720,0	43513,0
T1-6	13,0	4891,0	29599,9
T1-6	27,0	9595,4	18256,2
T1-6	29,0	3314,6	14175,7
T1-10	148,0	25498,7	42426,8
T1-10	149,0	20357,0	37629,6
T2-11	173,1	22154,2	27479,7
T2-11	174,1	28698,5	34541,1
T2-13	180,9	32257,1	33524,1
T2-13	181,8	35511,8	37089,5
T2-13	182,7	26615,9	32721,5
T2-13	183,6	37811,2	38615,4
T2-13	184,6	34526,2	36357,0
T2-13	185,6	24617,7	28989,9
T2-14	185,7	42112,2	44834,7
T2-14	186,7	38138,2	42477,6
T2-14	190,7	29407,9	34305,8
T2-12	191,7	37247,0	39175,1
T2-12	192,7	29300,5	30239,1
T2-12	193,7	27422,5	30456,5
T2-13	196,6	34961,2	41472,5
T2-13	197,6	40683,1	43624,3
T2-13	198,6	31766,2	41938,2
T2-13	199,6	37279,2	40855,5
T2-13	201,6	37279,2	40855,5
T2-13	202,3	40133,9	42676,8
n		30,0	30,0
min		3314,6	14175,7
max		45065,4	52589,6
average		29697,0	36127,7
stand.deviation		10314,6	8195,6
charact. value 90% (Fellin, 2005)		25245,4	32590,6

GT: 4b			
borehole	depth	E1	E2
T2-15	41,7	8918,3	30039,6
T2-15	43,1	10346,1	20781,2
T2-15	50,1	4593,6	24244,8
T2-15	51,1	10081,3	24670,6
T2-15	68,7	9711,0	32927,9
T2-15	69,0	1732,2	4422,0
T2-1	35,0	16906,5	
T1-3	4,0	9886,0	14828,6
T1-3	5,0		
T1-3	6,0	8012,0	15498,0
T1-1	7,0	12754,7	29362,1
T1-1	8,0	8715,1	19803,5
T1-1	9,0	3617,1	13038,4
T1-6	7,0	9162,0	17882,0
T1-6	8,0	7555,0	27122,0
T1-6	11,0	6749,9	16105,2
T1-6	12,0	7634,0	24412,0
T1-2	10,0	10417,3	17596,7
T1-2	11,0	11712,9	35735,4
T1-2	12,0	11631,1	35753,4
T1-3	11,0	20976,7	28083,0
T1-3	12,0	17920,9	39507,4
T1-6	14,0	8102,9	10775,6
T1-6	28,0	10394,8	17841,3
T1-10	80,0	9987,9	32724,0
T1-10	81,0	9960,8	21179,7
T1-10	82,0	4475,6	20280,7
T2-14	167,5	4526,6	10709,7
T2-14	168,3	4179,9	17176,0
T2-11	172,1	6180,7	15933,6
T2-14	187,7	5311,2	16989,7
T2-14	188,7	9396,1	24648,5
T2-12	189,2	6136,6	36336,8
T2-13	203,6	3956,1	34696,0
n		33,0	32,0
min		1732,2	4422,0
max		20976,7	39507,4
average		8837,7	22847,0
stand.deviation		4162,2	8779,7
charact. value 90% (Fellin, 2005)		7133,6	19191,1

GT:5a			
borehole	depth	E1	E2
T2-15	69,4	1732,2	4422,0
T2-15	77,2	1582,4	5490,3
T2-14	166,0	3912,2	
T2-13	203,0	3956,1	5014,2
T2-13	204,0	1090,6	10066,6
T2a-6	11,0	3139,0	9273,3
T2a-6	12,0	3766,5	7314,3
n		7,0	6,0
min		1090,6	4422,0
max		3956,1	10066,6
average		2739,9	6930,1
stand.deviation		1234,4	2345,6
charact. value 90% (Fellin, 2005)		2058,4	5068,5
charact.value vrednost 95% (Student)		1354,8	3900,8

GT: 5b			
borehole	depth	E1	E2
T2-08	100,0	2855,3	5518,7
T2-08	101,0	3384,3	5291,7
T2-1	37,0	1742,3	10094,4
T2-1	54,1	3684,4	7563,5
T2-1	55,0	3837,2	13585,1
T2-13A	170,0	2712,0	12888,0
T2-13A	169,0	3432,0	10582,0
T2-13A	179,0	2405,0	10277,0
T2-13A	179,8	2629,0	15670,0
n		9,0	9,0
min		1742,3	5291,7
max		3837,2	15670,0
average		2964,6	10163,4
stand.deviation		677,3	3565,7
charact.value vrednost 95% (Student)		2314,4	7934,2
charact. value 90% (Fellin, 2005)		2343,4	6893,0

0b			
borehole	depth	E1	E2
T1-15	6,0	375,6	466,7
T1-15	16,0	102,6	246,9
T1-13	5,0	49,1	216,3
T1-13	6,0	190,0	818,8
T1-15	17,0	261,8	326,3
T1-15	7,0	13,2	107,4
T1-15	11,0	26,9	138,0
n		7,0	7,0
min		13,2	107,4
max		375,6	818,8
average		145,6	331,5
stand.deviation		136,1	246,3
charact. value 90% (Fellin, 2005)		109,4	249,0

7. Poisson's ratio

A statistical analysis of the Poisson quotient was made on the base of measures of lab test results by grouping them into lithological units (Figure 25). For units 0a and 0b, where there were no lab measures, the values were determined on the base of experience and suggestions from the literature, as borehole as for units 5a and 5b, where the number of measures was too small and therefore not considered as statistically representative.

ν						
mean	max	min	st.dev.	RT	no.	95%
0,18	0,30	0,10	0,05	SSt	27,00	0,20
0,19	0,26	0,09	0,05	SM	10,00	0,23
0,19	0,32	0,09	0,09	Ma	9,00	0,26
0,18	0,32	0,10	0,06	lj	43,00	0,18
0,20	0,25	0,15	0,07	fm	2,00	0,11

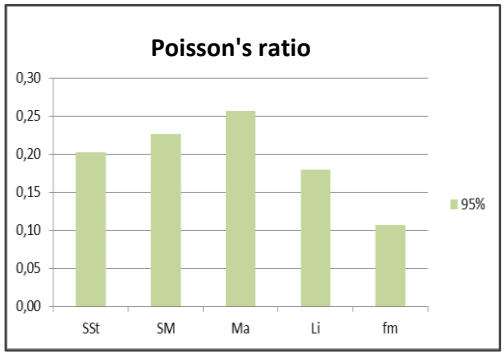

Figure 25: Results of the statistical analysis of the lab results vs. Poisson's ratio

Annex 3

Sketches of expected behaviour types – BTs

Behaviour type:	BT1 (limestone and flysch)

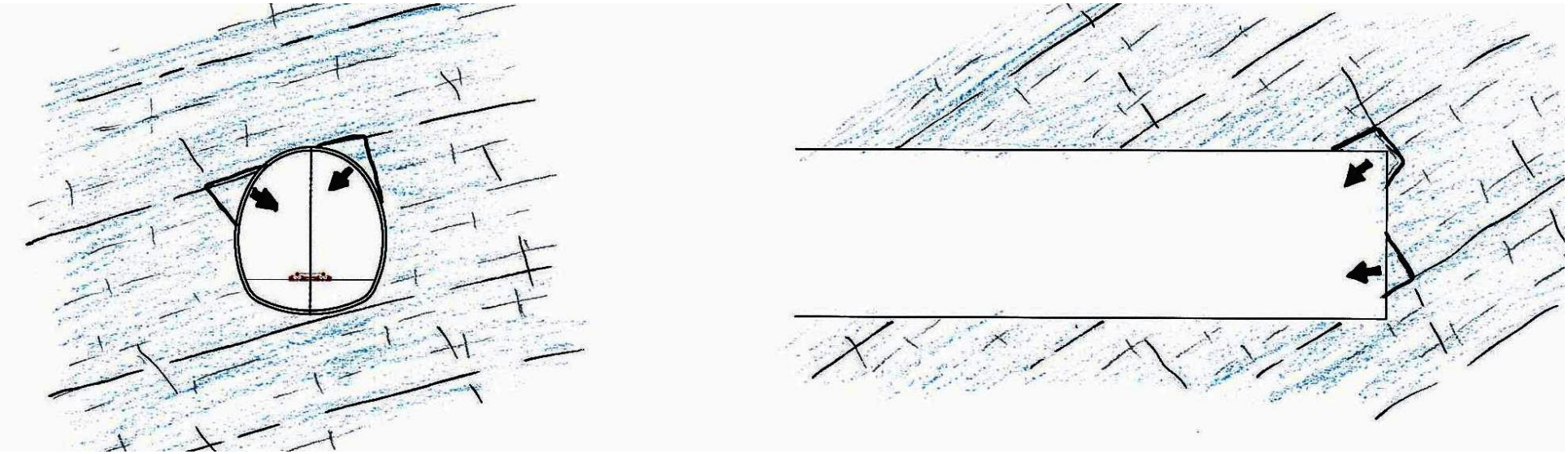

Ground type GT	Dominantly: 4a
Discontinuity orientation	Massive to thick layered limestones or thicker layers of compact sandstone with rare joints
Stresses	Rockmass strength exceeds stresses
Water inflow	Dry to damp along joints. In the area of flysch layers with limestone and in the area of fluctuations of groundwater, possible local point inflows 2-50 l/s.
Rockmass behaviour	Stable rockmass with the potential of local gravitational rockslides and rockfalls.

Behaviour type:	**BT2 (limestone)**

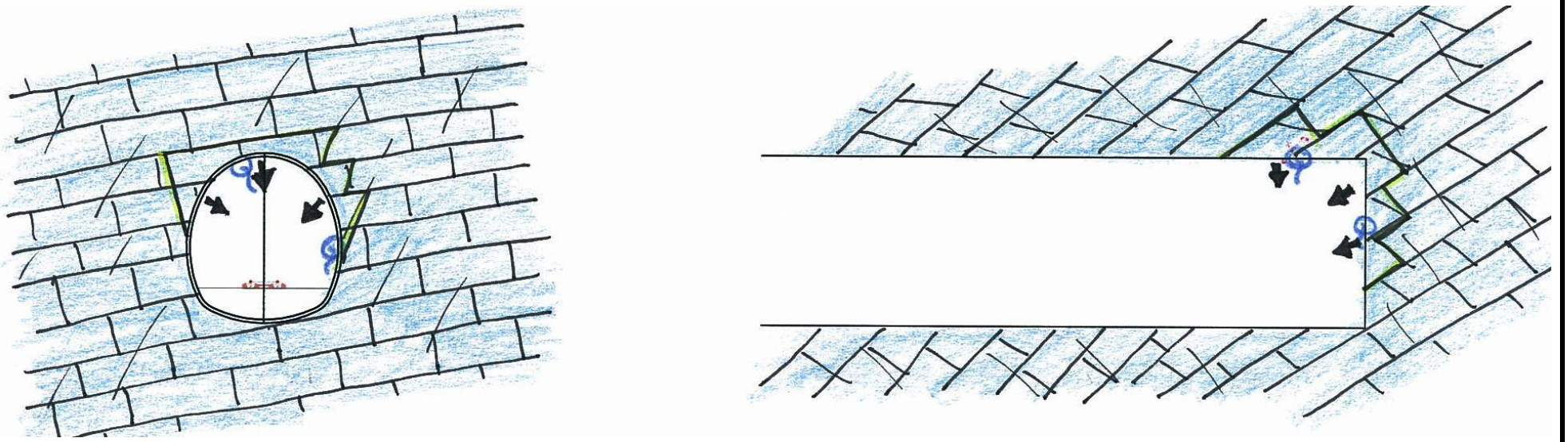

Ground type GT	Dominantly: 4a, 4b
Discontinuity orientation	Medium steep to steep layering, usually with dip against excavation, locally in excavation, can be folded along faults. Prevailing medium steep to steep joints with dip in excavation face, locally from excavation face.
Stresses	Rockmass strength usually exceeds stresses and always exceeds 80 % of stresses.
Water inflow	Locally possible temporary inflows.
Rockmass behaviour	Systematically discontinuities with large persistence, usually condition gravitational rockfall and ravelling of material. Rare shear failure. Local waterinflows can lower the shear strength along discontinuities. Waterinflow from interlayers can induce erosion processes, which can increase failure possibility. Medium to high possibility of block slides from excavation face.

Behaviour type:	BT3 (limestone)

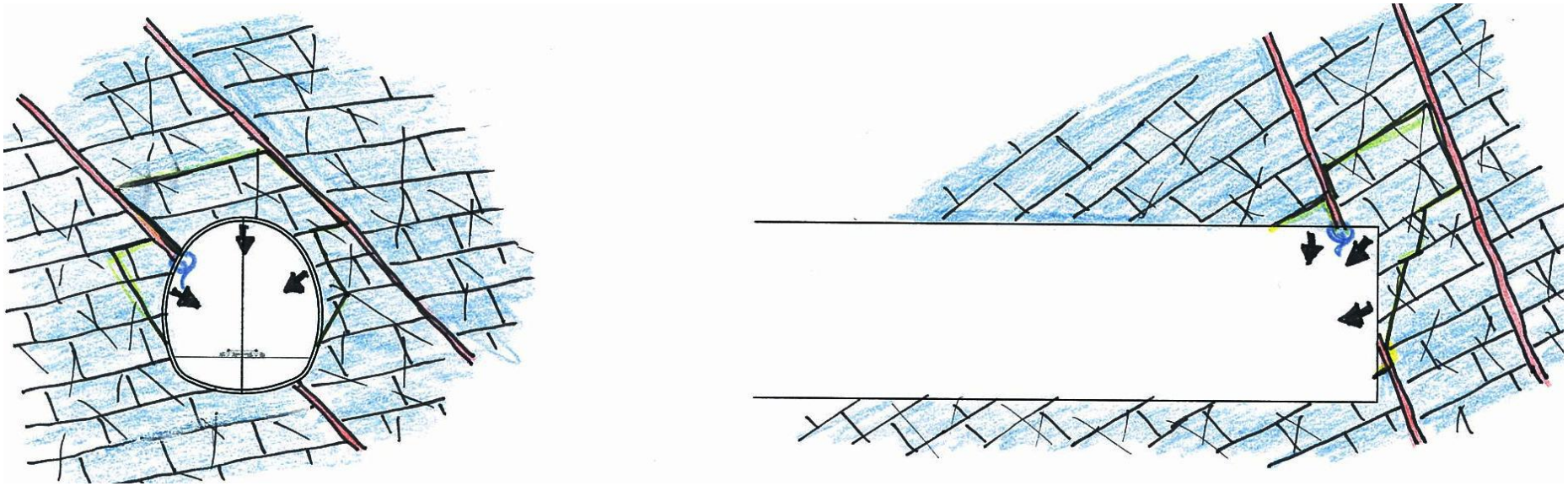

Ground type GT	Dominantly: 4b; subordinately 5a
Discontinuity orientation	Medium steep to steep layering, usually opposite of excavation, locally in excavation, can be folded along faults. Prevailing medium steep to steep joints with deep into excavation face.
Stresses	Rockmass strength exceeds stresses.
Water inflow	Water inflow from fracture zones can exceed 0,5 l/s. Along fault zone inflows of up to max. 2 l/s can occur.
Rockmass behaviour	Asymmetrical distribution of stresses in connection with shear zones, which can lead to local failures due to induced stresses. Relaxation creep along shear zones induces loosening, which increases the possibility of failures of greater dimensions. Waterinflow from interlayers can induce erosion processes, which can increase failure possibility.

Behaviour type:	BT4 (limestone)

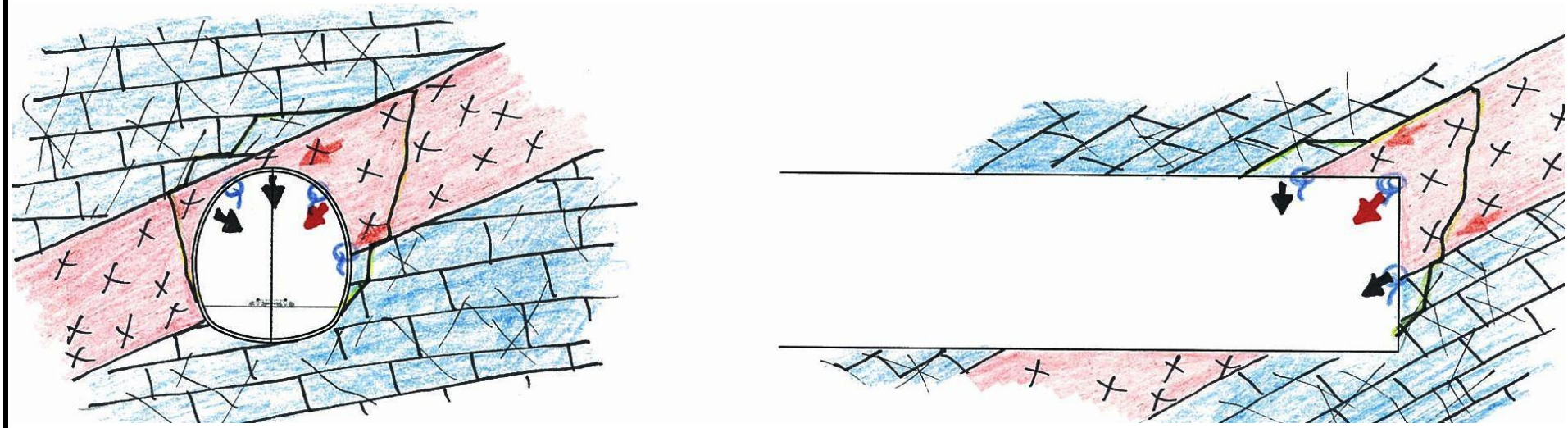

Ground type GT	Dominantly: 5a (GT5b - locally with fault limited bodies)
Discontinuity orientation	Prevailing medium steep (locally steep) dipping joints and shear joints, dipping mainly in excavation face. Layering dip is changing; medium steep to steep dips prevail. Partly chaotic structure.
Stresses	Stresses exceed rockmass strength. (*sigcm/po* ~ 0,15-0,50).
Water inflow	Water inflows from fracture zones can be up to 0,5 l/s. Inflows along faults can be up to 2 l/s.
Rockmass behaviour	Low rockmass strength in connection with relaxation and creep along shear zones can lead to deep failures. Failures can increase with waterinflow along shear zones and/or tectonic material. Occurrence of soil like tectonic material in connection with stiffer rockmass can lead to anisotropical rockmass behaviour. Large danger of deep failures.

Behaviour type:	BT7 (limestone-marl)

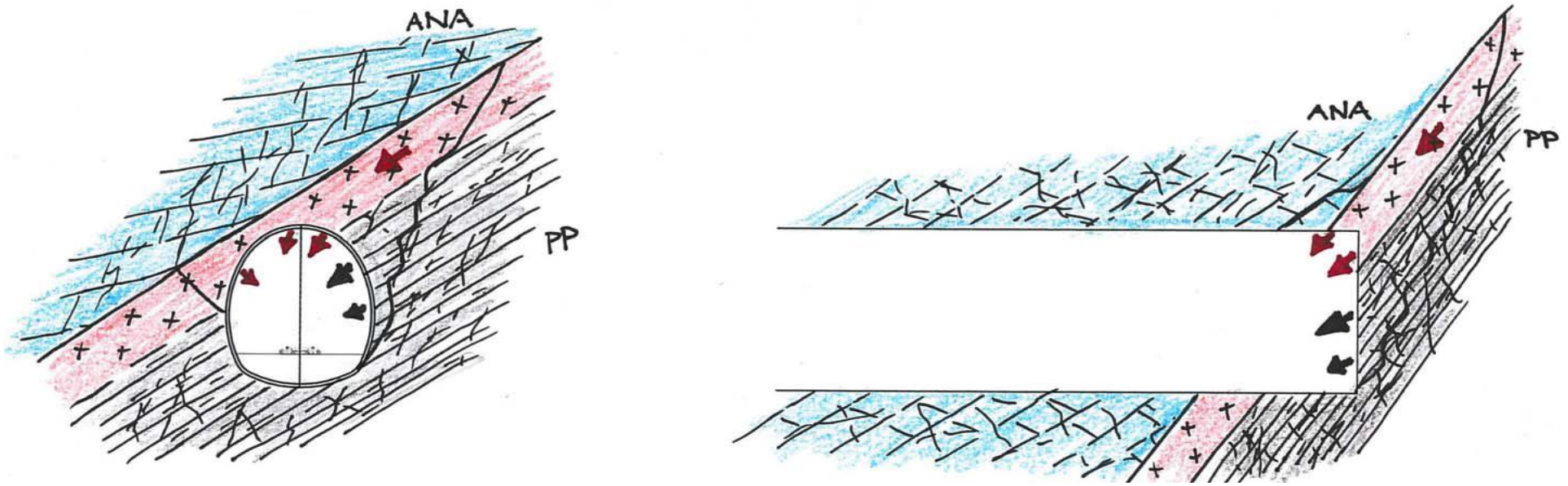

Ground type GT	Dominantly: 0a, 0b (5b-at limestone-marl contact)
Discontinuity orientation	Prevailing medium steep (locally steep) dipping joints and shear joints, dipping mainly in excavation face. Layering dip is changing, medium steep to steep dips prevail. Partly chaotic structure.
Stresses	Stresses exceed rockmass strength.
Water inflow	Locally possible temporary inflows of up to 2 l/s along fault zones and at contact.
Rockmass behaviour	Low rockmass strength in connection with relaxation and creep along shear zones can lead to deep failures. Failures can increase with waterinflow along shear zones and/or tectonic material. Occurrence of soil like tectonic material in connection with stiffer rockmass can lead to anisotropical rockmass behaviour. Large danger of deep failures.

Behaviour type:	**BT8 (limestone)**

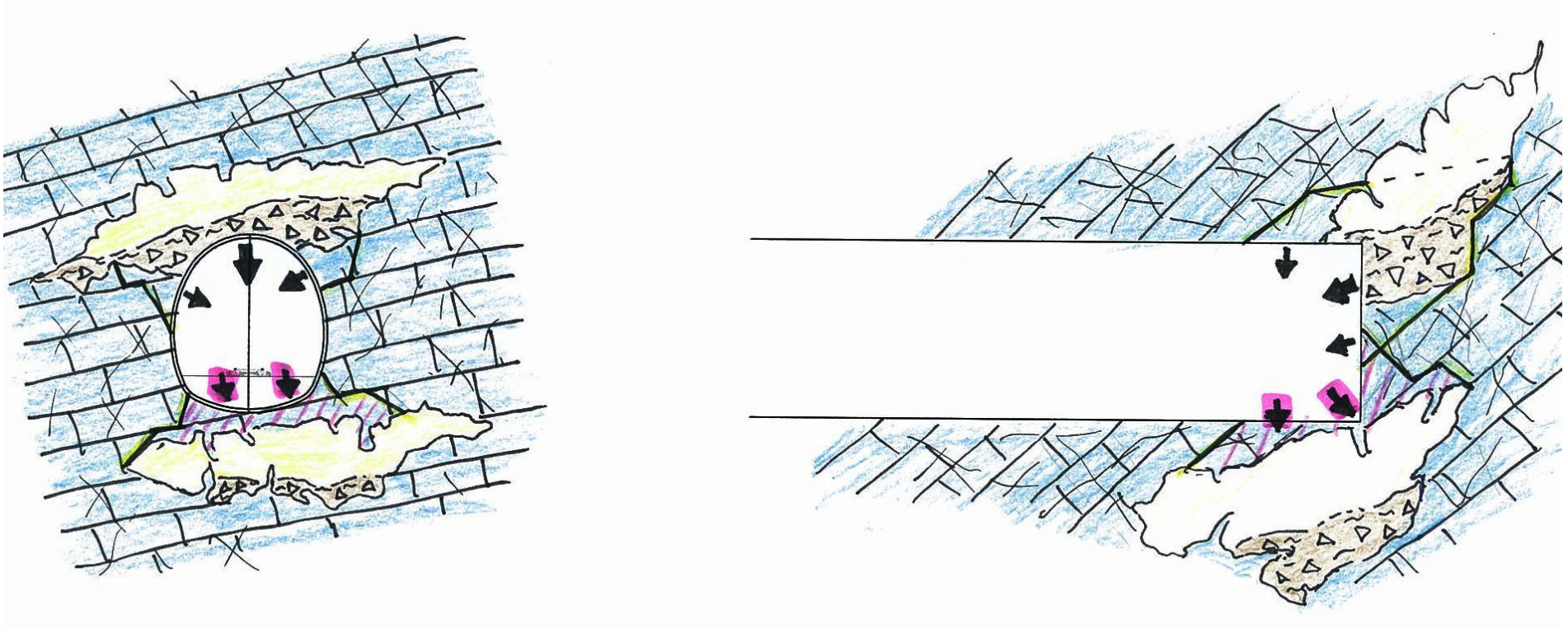

Ground type GT	GT4a, GT4b
Discontinuity orientation	Medium steep to steep layering, usually with dip against excavation, locally in excavation, can be folded along faults. Prevailing medium steep to steep joints with dip in excavation face.
Stresses	Stresses exceed rockmass strength.
Water inflow	Waterinflow can occur locally, from karstified areas, usually dry or damp.
Rockmass behaviour	Rockmass failure in the area of karstic features. Possible cavings and inflow of cave sediments (clayey gravel) and/or water in the excavation area due to karstic features above the excavation area or floor cavings of lower laying karstic caverns..

Behaviour type:	**BT2 (flysch)**

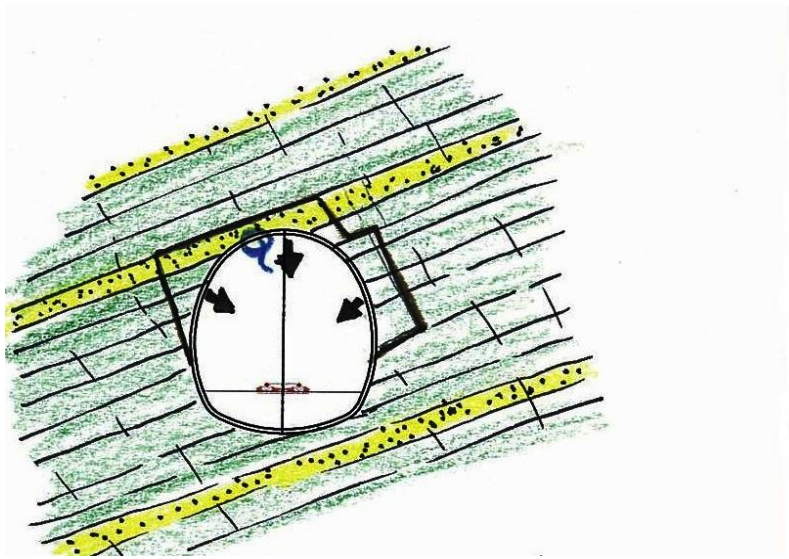

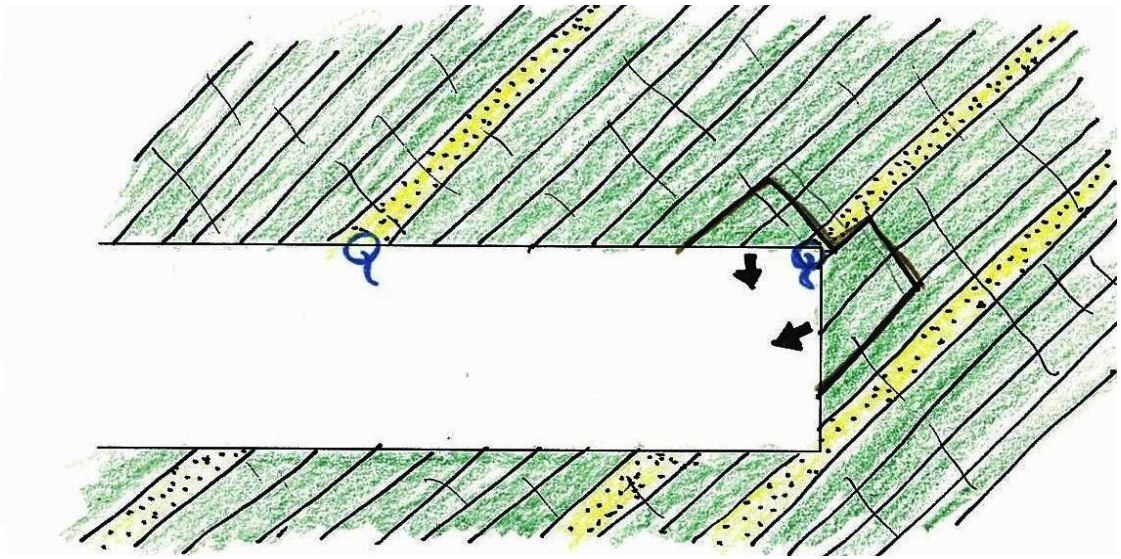

Ground type GT	Dominantly: 1a, 2a, 3a; subordinately 1b, 2b, 3b
Discontinuity orientation	Medium steep to steep layering, usually with dip against excavation, locally in excavation, can be folded allog faults. Previling medium steep to steep joints with dip from excavation face.
Stresses	Rockmass strength usually exceeds stresses and always exceeds 80 % of stresses.
Water inflow	Locally possible temporary inflows of up to 2 l/s along fault zones.
Rockmass behaviour	Systematically discontinuities with large persistence, usually condition gravitational rockfall and ravelling of material. Rare shear failure. Local waterinflows can lower the shear strength along discontinuities. Waterinflow from interlayers can induce erosion processes, which can increase failure possibility. Medium to high possibility of block slides from excavation face.

Behaviour type:	**BT3 (flysch)**

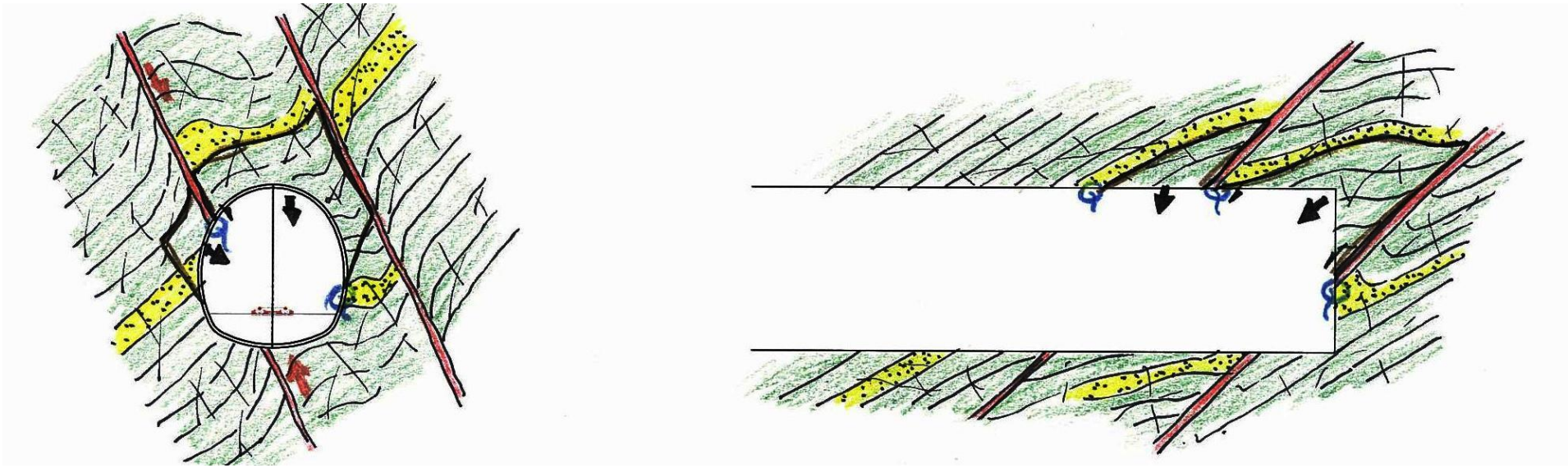

Ground type GT	Dominantly: 1b, 2b, 3b; subordinately: 5a
Discontinuity orientation	Medium steep to steep layering, usually with dip against excavation, locally in excavation, can be folded allog faults. Previling medium steep to steep joints with dip to and from excavation face.
Stresses	Stresses usually exceed rockmass strength.
Water inflow	Possible local inflows from sandstones, typically < 0,5 l/s. Inflows from fractured zones can exceed 0,5 l/s. Inflows of up to 2 l/s can occur along faults
Rockmass behaviour	Asymmetrical distribution of stresses in connection with shear zones, which can lead to local failures due to induced stresses. Relaxation creep along shear zones induces loosening, which increases the possibility of failures of greater dimensions. Waterinflow from sandstones can lower the shear strength along discontinuities and can induce erosion processes, which can increase failure possibility. High danger of block slides from excavation face.

Behaviour type:	BT4 (flysch)

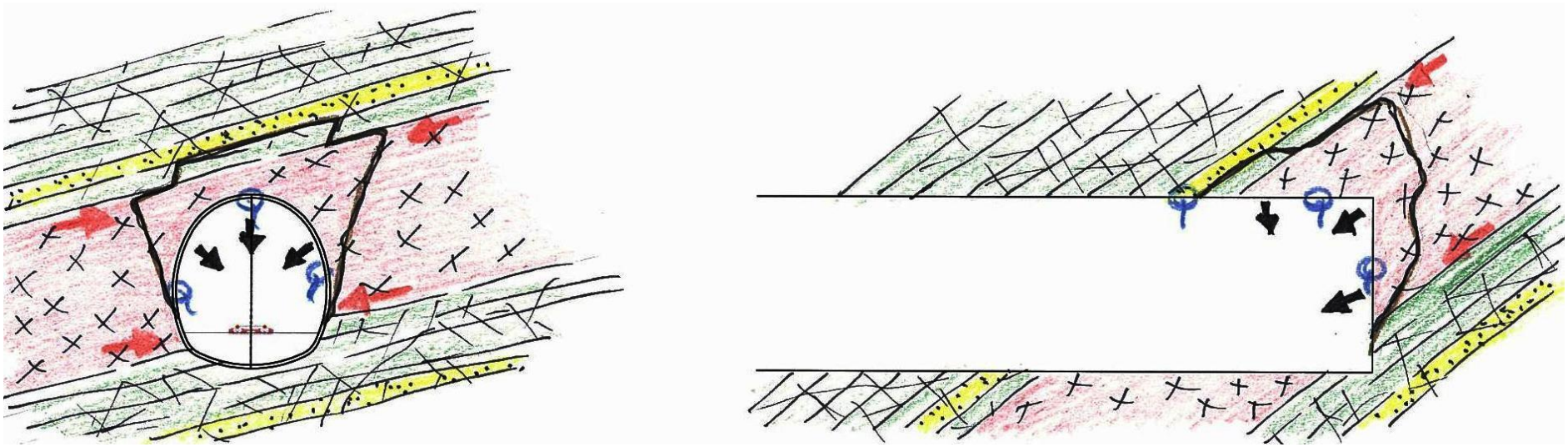

Ground type GT	Dominantly: 5a, 5b
Discontinuity orientation	Prevailing medium steep (locally steep) dipping joints and shear joints, dipping mainly from excavation face. Layering dip is changing; medium steep to steep dips prevail. Partly chaotic structure.
Stresses	Stresses usually exceed rockmass strength (*sigcm/po* ~ 0,15-0,50).
Water inflow	Local inflow from sandstone possible, typically < 0,5 l/s. Inflows from fractured zones can exceed 0,5 l/s. Inflows of up to 2 l/s can occur along faults.
Rockmass behaviour	Asymmetrical distribution of stresses in connection with shear zones, which can lead to local failures due to induced stresses. Relaxation creep along shear zones induces loosening, which increases the possibility of failures of greater dimensions. Waterinflow from sandstones can lower the shear strength along discontinuities and can induce erosion processes, which can increase failure possibility. High danger of block slides from excavation face.

Behaviour type:	BT7 (flysch)

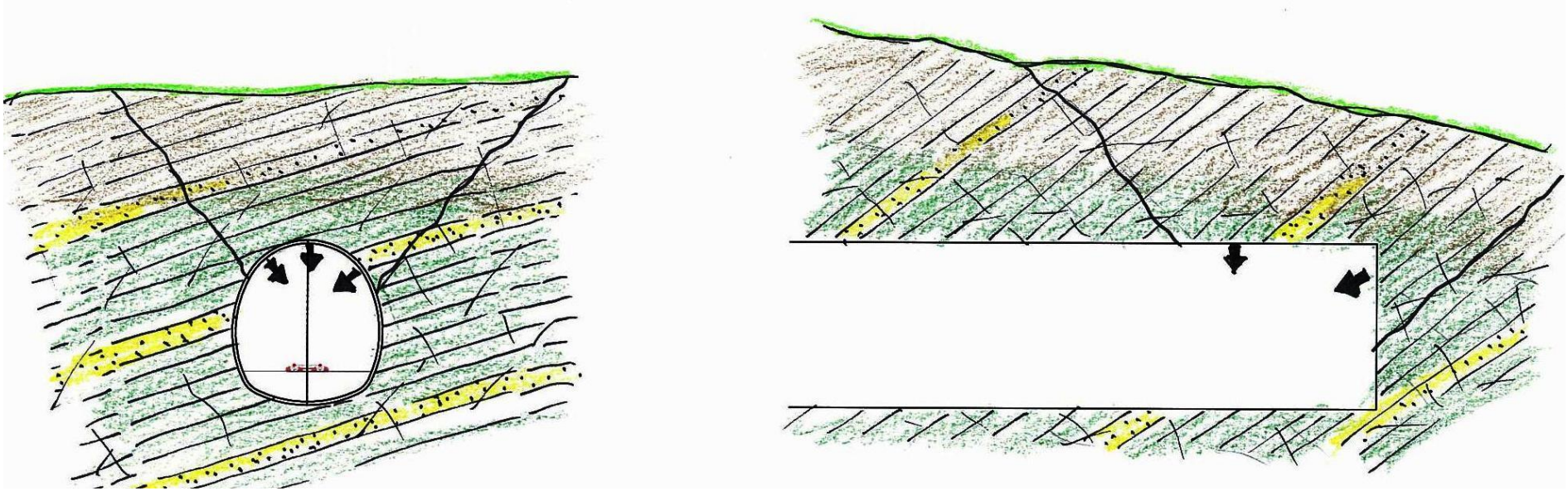

Ground type GT	Dominantly: 0a, 0b (GT1b, GT2b, GT5b - locally possible; fault limited bodies and at low overburden)
Discontinuity orientation	Medium steep to steep layering, usually with dip against excavation direction, locally in excavation direction, can be floded along faults. Prevailing medium steep to steep joints with dip from excavation face.
Stresses	Stresses usually exceed rockmass strength (*sigcm/po* < 0,15).
Water inflow	Usually dry to damp.
Rockmass behaviour	Ravelling of heavily fractured, locally soil-like rockmass with low cohesion. Ravelling in connection with low rockmass strength and limited lateral pressure can lead to fast progressive failures.